



Generative adversarial networks in medical image reconstruction: A systematic literature review



Jabbar Hussain ^{a,*}, Magnus Båth ^b, Jonas Ivarsson ^a

^a Dept. of Applied IT, University of Gothenburg, Forskningsgången 6, 417 56, Sweden

^b Department of Medical Radiation Sciences, University of Gothenburg, Sweden

ARTICLE INFO

Keywords:

Generative adversarial networks
Image reconstruction
Medical image processing
Deep learning
Modality

ABSTRACT

Purpose: Recent advancements in generative adversarial networks (GANs) have demonstrated substantial potential in medical image processing. Despite this progress, reconstructing images from incomplete data remains a challenge, impacting image quality. This systematic literature review explores the use of GANs in enhancing and reconstructing medical imaging data.

Method: A document survey of computing literature was conducted using the ACM Digital Library to identify relevant articles from journals and conference proceedings using keyword combinations, such as “generative adversarial networks or generative adversarial network,” “medical image or medical imaging,” and “image reconstruction.”

Results: Across the reviewed articles, there were 122 datasets used in 175 instances, 89 top metrics employed 335 times, 10 different tasks with a total count of 173, 31 distinct organs featured in 119 instances, and 18 modalities utilized in 121 instances, collectively depicting significant utilization of GANs in medical imaging. The adaptability and efficacy of GANs were showcased across diverse medical tasks, organs, and modalities, utilizing top public as well as private/synthetic datasets for disease diagnosis, including the identification of conditions like cancer in different anatomical regions. The study emphasized GAN’s increasing integration and adaptability in diverse radiology modalities, showcasing their transformative impact on diagnostic techniques, including cross-modality tasks. The intricate interplay between network size, batch size, and loss function refinement significantly impacts GAN’s performance, although challenges in training persist.

Conclusions: The study underscores GANs as dynamic tools shaping medical imaging, contributing significantly to image quality, training methodologies, and overall medical advancements, positioning them as substantial components driving medical advancements.

1. Introduction

In recent years, there has been significant growth in the field of medical image-based diagnosis and treatment, aided by computer models using machine learning techniques [1–4]. Medical imaging data are collected through various techniques, including conventional radiography [5], computed tomography (CT [6]), and magnetic resonance imaging (MRI [7]), among others approaches, providing detailed, noninvasive anatomical information. Each medical imaging technique leverages signals from different bands of the electromagnetic spectrum, some of which overlap in frequency but involve different physical processes. Such as X-rays (used in conventional radiography, and CT), gamma rays (in positron emission tomography, PET, and single-photon

emission tomography, SPECT), infrared radiation (in thermal imaging), radiofrequency (RF; in nuclear MRI), and visible light (in microscopy, and endoscopy), among others. Additionally, pressure sound waves are used in ultrasound imaging (US [8]).

Despite these technological advancements, medical images are often corrupted by factors, such as noise, motion blur, and/or missing information, making it difficult to obtain high-quality images. For instance, chest tomosynthesis (CTS [9]), an acquisition technique, collects data from a limited range of angles (rather than a full rotation like CT), and reconstructs the 3D anatomy into a stack of images. The limited-angle acquisition results in incomplete internal anatomical data for 3D reconstruction, making it challenging to achieve image quality comparable to that of standard CT scans. This raises the question of how to fill

* Corresponding author.

E-mail address: jabbar.hussain@ait.gu.se (J. Hussain).

the gap of lost information. Despite this limitation, CTS has the potential to reduce costs and radiation exposure for patients while maintaining diagnostic accuracy. Traditional CT reconstruction algorithms appear insufficient for this task. Since the anatomy of the human body is well constrained, it may be possible to reconstruct a 3D image using deep learning algorithms,—in particular, generative adversarial networks (GANs)—have been critical in advancing this area and have become increasingly popular since their inception [10]. GANs have been utilized for cross-modality image transfer, and their effectiveness has been demonstrated in various studies [11,12]. GANs have been applied to a variety of image processing tasks, such as image synthesis [13], image translation [14], image/semantic segmentation [15,16], image/data generation, classification [17,18], text to photo-realistic image synthesis [19], and domain adaptation [11,12], among others.

GANs have also shown great promise in medical image reconstruction, allowing for the generation of high-quality images from low-quality or incomplete data. GANs have been used to reconstruct 3D images from 2D data [20], improving image structural consistency loss, remove noise [21], and eliminate artifacts [22] in medical images. Despite these advantages, GANs also face certain limitations, such as the potential for overfitting, and the need for large amounts of training data. Medical image reconstruction is a process of converting signals acquired from various sensors into images that can be utilized to study and diagnose biological processes in cell and organs tissues [8]. To gain a comprehensive understanding of GANs, and their applications in enhancing or reconstructing medical imaging data, a systematic literature review is essential. We anticipate that such a review will offer valuable insights to guide both novice and experienced researchers in selecting appropriate research topics and developing suitable methodological approaches within the studied subject. The key contributions of this article are:

- It offers a systematic literature review to investigate the prevalence of GANs in enhancing or reconstructing medical imaging data.
- It provides valuable insights into the application of GANs across multiple dimensions, including the tasks performed, the organs served, yearly trends in GAN applications, modality-specific uses, uses in image reconstruction, and the datasets and evaluation metrics employed in the reviewed studies.
- It outlines potential future research directions.

This review uncovers GANs as dynamic tools in medical imaging, suggesting their potential as important contributors to progress in medical advancements. Looking ahead, GANs may also significantly contribute to diagnosing diseases and detecting anomalies, particularly identifying conditions such as cancer across different anatomical regions. This implies that future research should prioritize ethical considerations and the responsible use of artificial intelligence and machine learning (AI&ML) models.

The following subsections offer an overview of relevant surveys, explore medical imaging modalities, and highlight the limitations of this review.

1.1. Related surveys

In recent years, image reconstruction techniques have undergone a paradigm shift, transitioning from traditional analytical approaches to iterative methods, and more recently, to machine learning-based approaches. These data-driven methods either map raw sensory data inputs directly into output images or serve as post-processing tools to enhance image quality by addressing challenges such as noise, motion blur, missing information, or eliminating artifacts that compromise image quality. These techniques enable clinicians to obtain clear, accurate visualizations of internal structures within the human body, facilitating more accurate diagnosis and treatment of diseases.

Among these methods, the most promising techniques are GANs,

which serve as robust tools for constructing deep networks capable of addressing domain shift or bias in training data through adversarial learning [23]. Several surveys have examined the applications of GANs in medical image processing, shedding light on their potential and challenges. For instance, Yi et al. reviewed advancements in medical imaging using adversarial training, highlighting the nascent integration of GANs into the field and the lack of clinical applications for GANs-based methods [24]. Jeong et al. explored recent trends in applying GANs to clinical diagnosis, particularly in medical image segmentation and classification [25]. Iqbal et al. conducted a comprehensive survey of the application of GANs in medical image segmentation, examining various facets of their application [26]. They emphasized the expectation of developing more effective GAN-based networks to address challenges in biomedical image segmentation and enhance real-world computer-aided diagnosis systems. Xun et al. demonstrated that using GANs and their variants improves the accuracy of medical image segmentation, while emphasizing the importance of rigorous verification, including testing generalizability in real, out-of-distribution datasets [27]. Chen et al. conducted a systematic review of medical image augmentation, highlighting the role of GAN-based methods in addressing the challenge of limited training samples for diagnostic and treatment models [28]. Ferrante et al. surveyed slice-to-volume registration, categorizing various algorithms while evaluating their strengths and weaknesses [29]. They suggested that transitioning to a learning-based approach for slice-to-volume registration could improve both speed and accuracy. Wang et al. summarized the current state and future potential of GANs, emphasizing their role as powerful generative models in parallel systems research (parallel intelligence) [30]. Cahyawijaya et al. surveyed biomedical image reconstruction, examining current trends in deep learning-based approaches [31]. They suggested that future research could explore emerging techniques such as hourglass architecture, transformer architecture, and self-supervised pre-training, in biomedical image reconstruction. Finally, Ben et al. reviewed state-of-the-art image reconstruction algorithms, focusing on deep learning methods, and highlighted future research directions to improve image quality under resource constraints [8]. **Table 1** provides a comparative analysis of selected state-of-the-art surveys on GANs within the context of medical image processing. The analysis encompasses datasets, metrics, radiology modality, organs served, loss function, task investigated, research objectives, and recommendations for future research or remarks. These reviews emphasize the significant role of GANs in areas such as segmentation, classification, augmentation, image registration, and reconstruction. However, there is a notable gap in the literature regarding the application of GANs to image reconstruction, particularly in cases where limited-angle acquisition leads to incomplete anatomical data, hindering the generation of high-quality images. Therefore, a systematic literature review is essential to gain a comprehensive understanding of GAN's applications in enhancing or reconstructing medical imaging data. It is also valuable to understand and explore different medical imaging modalities, which are discussed in the following subsection.

1.2. Image modality

A medical imaging modality refers to a technique utilized to generate visual representations of internal organs within the human body, primarily to aid in the diagnosis, modeling, or treatment of diseases. These visual representations are created by utilizing physical phenomena, including radioactivity, electromagnetic radiation, sound, nuclear magnetic resonance, among others. Medical imaging modalities can be categorized into anatomical and functional types. Anatomical imaging methods, such as conventional radiography [5], CT [6], and MRI [7], provide detailed information about the structure of the body. In contrast, functional modalities, such as SPECT [32], PET [33], functional magnetic resonance imaging (fMRI [34]), and angiography [35], offer insights into the functioning of organs. Different medical imaging

Table 1

Comparative analysis of state-of-the-art GAN surveys.

Published works	Duration	Datasets public (P) private (S)	Evaluation metrics	Radiology modality	Organs serverd	Loss function	Tasks count	Task investigated	Research objectives	Remarks
Yi et al. [24]	2014 - Jan 1, 2019	P&S	x	x	x	x	6	CT denoising, cross-modality transfer (vessels to fundus), skin lesion synthesis, domain adaptation, abnormality detection.	Reviewed recent advances in medical imaging using adversarial training, offering insights for researchers.	Despite promising results, the use of GANs in medical imaging is still in its early stages, with no major clinical applications yet.
Ben et al. [8]	2010–20	P&S	x	x	x	x	1	Reconstruction	Reviewing cutting-edge image reconstruction algorithms, focusing on DL-based methods, to identify future research opportunities.	Future advancements aim to produce higher-quality images with constrained resources.
Cahya-wijaya [31]	–	P	x	x	x	x	1	Reconstruction	This survey helps machine learning researchers understand the field and current trends in deep biomedical image reconstruction.	Future work could explore trending approaches such as hourglass and, transformer architecture, and self-supervised pre-training, and their combinations, in biomedical image reconstruction.
Jeong et al. [25]	Jan 2015–Aug 2020	P&S	x	x	x	x	2	Classification & Segmentation	A review exploring recent trends in GAN applications for clinical diagnosis, with a focus on medical image segmentation, classification, and task-based implementations.	State-of-the-art GAN methods for medical images need rigorous verification, including testing generalizability on real, out-of-distribution datasets, beyond expert visual inspection.
Xun et al. [27]	Until Sep 2021	P&S	x	x	x	x	1	Segmentation	Authors claim that using GAN and its variants improves medical image segmentation accuracy.	Gaining clinician and patient trust in GAN methods is challenging due to issues like instability and low repeatability, which must be addressed for further development.
Iqbal et al. [26]	Jan 2016–Mar 2021	P&S	x	x	x	x	1	Segmentation	Surveying GAN applications in medical image segmentation, covering models, metrics, loss functions, datasets, augmentation, implementations, source codes, and their role in human disease segmentation.	Developing effective GAN-based networks is essential for tackling challenges in biomedical image segmentation and enhancing computer-aided diagnosis systems.
Chen et al. [28]	2018–21	P&S	x	x	x	x	1	Augmentation	Conducting a systematic review of GAN-based medical image augmentation, focusing on its current research status and future prospects.	GAN-based medical image augmentation helps overcome the challenge of limited training samples in medical diagnosis and treatment models.
Ferrante et al. [29]	–	P&S	x	x	x	x	1	Registration	Conducting a survey on slice-to-volume registration, categorizing algorithms by an adhoc taxonomy, and analyzing the pros and cons of each category.	The authors suggest that transitioning to a learning-based slice-to-volume registration could improve speed and accuracy, offering new possibilities in the field.
Wang et al. [30]	2014 - 2016/17 (Unclear)	P&S	–	–	–	x	–	–	Summarizing GAN's current state and future potential in parallel	GANs, as powerful generative models, can

(continued on next page)

Table 1 (continued)

Published works	Duration	Datasets	Evaluation metrics	Radiology modality	Organs served	Loss function	Tasks count	Task investigated	Research objectives	Remarks
This review	Until 31st Aug 2023	P&S	x	x	x	x	1	Reconstruction	systems research (parallel intelligence). The research explores the prevalence of GANs in medical image reconstruction.	integrate into the study of parallel intelligence. Future research should prioritize ethical considerations, responsible AI/ML use, and the use of open datasets for external validation.

modalities serve distinct purposes, each with specific strengths and limitations [36]. For instance, CT is particularly effective at distinguishing tissues with different densities, such as bones and blood vessels, while MRI is best for visualizing soft tissues like the abdomen and liver [36]. PET images provide functional information related to metabolism, but they are often pseudo-colored and have low resolution [36]. Mammograms, which use low-energy X-rays, are essential for breast screening and diagnosis [37]. In ophthalmology, optical coherence tomography (OCT) provides non-invasive cross-sectional imaging to detect ocular diseases such as macular edema, while fundus imaging captures direct visual information, depicting anatomical structures such as the optic disc and vasculature [38]. The information portrayed in medical images acts as a reflection of the body's status [36].

Recent advancements have integrated deep learning into medical image processing, including enhancing and reconstructing images across various modalities. Applications span CT, MRI, PET, ultrasound systems, optical microscopy, photo acoustic tomography (PAT), fluorescence microscopy, electromagnetic tomography (EMT), diffuse optical tomography, monocular colonoscopy, holographic image reconstruction, reconstruction of neural volumes, stochastic microstructure reconstruction, coherent imaging systems, tomographic 3D reconstruction of a single-molecule structure, neutron tomography, and the integration of deep learning with transfer learning in imaging [76]. The choice of modality depends on the required diagnostic information and the energy source used.

1.3. Limitations of the review

This review focuses exclusively on the use of GANs for the "image reconstruction task" in medical image processing. It examines papers published from GAN's formal introduction in 2014 to August 31, 2023, with an additional six-month buffer to ensure a comprehensive review of relevant studies. Although the analysis, limited to the ACM Digital Library databases, may not have been exhaustive, it is expected that these studies will provide sufficient knowledge to aid both novice and experienced researchers in selecting research topics and refining methodological approaches within the studied subject.

The survey is organized as follows: Section 2 discusses diffusion-based generative models, section 3 covers the concepts of GANs, section 4 outlines the research methodology, section 5 presents the results and discussion, section 6 concludes the study, section 7 lists the references, and section 8 includes the appendices.

2. Generative models

The field of generative models encompasses the following primary categories: variational autoencoders (VAEs), generative adversarial networks (GANs), autoregressive networks, and diffusion models. Among these deep learning models, diffusion models and GANs have

garnered substantial attention in the domain of image processing. Diffusion model is described below.

2.1. Diffusion models:

Image reconstruction using deep learning involves employing deep neural networks to generate or restore high-quality images from degraded or low-resolution inputs. These algorithms are designed to transform collected signals into two-, three-, or four-dimensional representations. Among these methods, diffusion models—recognized as one of the effective generative models—have emerged as significantly versatile tools in the domain of image processing. The concept of diffusion models was first introduced by Jascha Sohl-Dickstein et al. in their seminal work "*Deep Unsupervised Learning Using Nonequilibrium Thermodynamics*" [58]. The approach gained prominence with the contribution of Jonathan Ho et al. in their paper "*Denoising Diffusion Probabilistic Models*," which highlighted its potential for image generation tasks [59]. A diffusion model operates through two main processes: a forward process and a inverse (or reverse) process. In the forward process, noise is incrementally added to the input data over a Markov chain of diffusion steps until it becomes indistinguishable from random noise. The reverse process, trained to reverse this degradation, learns to reconstruct the original data by progressively removing the added noise. This model facilitating tasks such as denoising and inpainting [59].

Recent advancements in diffusion models have significantly impacted image processing. For instance, Güngör et al. introduced AdaDiff, a diffusion-based MRI reconstruction method, demonstrating superior performance in cross-domain tasks while also performing competitively in within-domain tasks [60]. Özbeş et al. proposed SynDiff, an adversarial diffusion model for medical image translation, showing superior performance in multi-contrast MRI and MRI-CT tasks [61]. Wu et al. developed the Multi-channel Optimization Generative Model (MOGM) for ultra-sparse-view CT reconstruction, achieving significant results through novel data consistency and multi-channel fusion [62]. Zhang et al. introduced the Wavelet-Inspired Score-based Model (WISM) for limited-angle CT (LA-CT) reconstruction, demonstrating superior performance with robust results [63]. Wu et al. also proposed a wavelet-based denoising technique to improve score-based generative models (SGMs) for CT and MRI reconstructions [64]. The versatility and efficacy of diffusion models continue to position them as significant tools in image processing research. In the next section, we will focus on GAN, as this article aims to investigate GAN for image reconstruction tasks.

3. Generative adversarial networks

GANs have attracted significant attention for their ability to effectively model complex real-world data. Introduced by Goodfellow et al. (2014) [10], GANs have demonstrated notable success in generating

synthetic data that closely resemble real-world data.

3.1. Types of GANs

There are several types of GAN algorithms exist, each with its unique architecture and training methodology. The following are some of the popular GAN algorithms:

Joo et al. proposed a GAN-based network that generates fusion images by transforming an object or person into a desired shape, combining the identity of one image with the shape of another [12]. This network has demonstrated qualitative results on datasets such as MPIIGaze [39], UnityEyes [40], and the Photo-Sketch-Cartoon dataset. Isola et al. investigated conditional adversarial networks (cGANs) as a general-purpose solution for image-to-image translation problems [41]. The cGANs accept various types of conditional inputs, including an attribute vector, a text description, or an image, and generate an output image using techniques like attribute-to-image generation, text-to-image generation [42], or image-to-image translation [41,43]. Ledig et al. introduced the super resolution GAN (SRGAN), which produces significantly more photo-realistic reconstructions for large upscaling factors ($4\times$) compared to other state-of-the-art reference methods [44]. Perarnau et al. proposed the Invertible cGAN (IcGAN) for regenerating real images with deterministic complex modifications [45]. Zhu et al. introduced CycleGAN, an approach for unpaired image-to-image translation [43]. ModularGAN enables the generation of multidomain images and facilitates image-to-image translation [46]. StyleGAN specializes in generating high-resolution headshots of fictional individuals, capturing attributes such as facial pose, freckles, and hair [47]. Motamed et al. introduced RandGAN, a method designed for detecting COVID-19 in chest X-ray images [48]. Li et al. introduced ObjGAN, which understand captions, sketches layouts, and refines details from text descriptions [49]. In summary, GANs are powerful tools for generating synthetic data that closely resemble real-world data. With their diverse architectures and training methodologies, various types of GAN algorithms can effectively address a wide range of applications.

3.2. Architecture of GAN

GAN architecture consists of two components: the generator and the discriminator [10]. These components engage in a zero-sum game, where a gain for one agent results in a loss for the other. Both components are trained simultaneously in an adversarial manner. The process begins by feeding an input vector to the generator. The generator's role is to create artificial or fake images that closely resemble real images. These generated images are then passed to the discriminator, which attempts to classify them as either real or fake. The generator's goal is to fool the discriminator by producing fake images that are as similar as possible to real ones. Meanwhile, the discriminator is trained to distinguish between real and fake images. If the discriminator correctly

identifies the fake image, it sends feedback to the generator, prompting it to adjust its weights to create more realistic images. If the discriminator makes an incorrect decision, it is updated to enhance its ability to detect fake images. This process continues iteratively until both the generator and discriminator reach an optimal state, where the generator produces highly realistic images, and the discriminator achieves maximum accuracy in distinguishing real from fake. GANs are probably best known for their contribution to image and video synthesis, artwork, music, speech, medicine, robotics, deepfake detection, and future directions, and other fields. However, GANs have certain drawbacks, such as the potential for the generator and discriminator to overpower each other. If the generator becomes excessively accurate, it can lead to undesirable outcomes. Conversely, if the discriminator becomes too precise, it may hinder the generator's progress toward convergence. Fig. 1 illustrates the basic architecture of a GAN model. The structure of GANs may vary depending on the application domain and specific needs. Several GAN extensions have been proposed in the literature, including conditional GANs, deep convolutional GANs, and progressive GANs, among others.

3.3. Loss functions in GANs

The GAN [10] has two primary loss functions: the generator loss and the discriminator loss. The generator loss quantifies how effectively the generated data fools the discriminator into classifying it as real. A lower generator loss indicates that the generator is producing more realistic data. The discriminator loss measures the discriminator's ability to differentiate real data from generated (fake) data. A lower discriminator loss indicates that the discriminator is effectively identifying fake data. The objective function of GAN represents the overall function being optimized during the training process, typically characterized by a min-max loss structure [10]. This min-max loss function serves as the performance metric for both the generator G and the discriminator D , guiding their learning processes. The G seeks to minimize the min-max loss, while the D aims to maximize it. The minimax game for two players, G and D , with value function $V(G, D)$, is given by equation (1).

$$\min_G \max_D V(D, G) = E_{x \sim p_{\text{data}}(x)} [\log D(x)] + E_{z \sim p_z(z)} [\log (1 - D(G(z)))] \quad (1)$$

In the min-max loss function, \min_G denotes the minimization of the loss function with respect to the G , while \max_D represents the maximization of the loss function for the D . The values function $V(D, G)$ represents the overall loss, considering both the G and D . The expectation operator E_x computes the average value of a function over the data distribution, considering all possible data points and their probabilities. E_x refers to the expectation over the real data distribution x , and E_z represents the expectation over the random noise distribution z . The term $\log D(x)$ measures the D 's loss when presented with real data x , where a higher

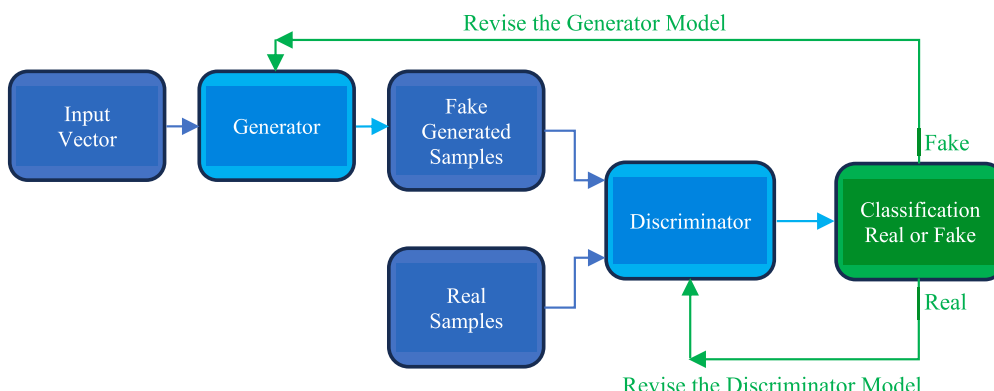


Fig. 1. The fundamental structure of a generative adversarial network model.

log value indicates a low loss for the D , ideally close to 1 for real data. Here, $G(\mathbf{z})$ represents the G 's output given the noise input \mathbf{z} , $D(\mathbf{x})$ is the D 's probability that real data \mathbf{x} is real, and $D(G(\mathbf{z}))$ is the D 's probability that the synthetic data $G(\mathbf{z})$ is real. Finally, E_x and E_z denote the mean likelihoods over all real and synthetic data, respectively. The generator and discriminator losses are defined by equations (2) and (3):

$$L_{\text{gen}} = E_{\mathbf{x} \sim p_{\text{data}}(\mathbf{x})} [\log (1 - D(G(\mathbf{z})))] \quad (2)$$

$$L_{\text{disc}} = -E_{\mathbf{x} \sim p_{\text{data}}(\mathbf{x})} [\log D(\mathbf{x})] - E_{\mathbf{z} \sim p_z(\mathbf{z})} [\log (1 - D(G(\mathbf{z})))] \quad (3)$$

Where $\log(D(\mathbf{x}))$ is the probability that the discriminator correctly identifies the real image and the $\log(1 - D(G(\mathbf{z})))$ helps discriminator to correctly label the fake image generated by the generator. In addition to the primary loss functions, GANs can also integrate auxiliary information to the loss function to improve training stability or promote specific properties in the generated samples. This may involve feature matching loss, reconstruction loss, gradient penalty loss, among others. The choice and combination of loss functions in GANs can vary depending on the specific GAN variant, application domain, and desired objectives. Different loss functions emphasize certain aspects of the training objective, such as sample quality, discriminator performance, or desired properties in the generated samples.

3.4. Challenges in GAN training

In GAN the training process aims to find an equilibrium where the generator produces high-quality samples that deceive the discriminator, while the discriminator becomes more adept at distinguishing between real and generated samples. It is crucial for GANs to reach the Nash equilibrium during training, but this is not a straightforward task. The training dynamics of GANs have been recognized as unstable [50]. The main factors contributing to this instability include mode collapse, convergence issues, and vanishing gradients. These challenges remain significant concerns in GAN research [51].

The mode collapse in a GAN occurs when the generator fails to capture the full diversity and variability of the target data distribution [50]. This issue can be addressed through two approaches: the objective function approach [52] and the structural approach *packing* [53]. The convergence happens when both networks reach equilibrium, where the generator can no longer significantly improve its output quality, and the discriminator achieves a high level of discrimination accuracy. Researchers have employed techniques such as architectural modifications [54], regularization methods [55,56], and optimization strategies [56] to enhance convergence and improve overall GAN performance. Despite these efforts, consistent convergence behavior remains elusive in GAN training. The vanishing gradients in GAN training refer to a phenomenon where the gradients used to update network parameters during the backpropagation process become extremely small or effectively vanish as they propagate through the network layers. For instance, minimizing the objective function (such as minimax) of GANs [57] can result in vanishing gradient problems. To mitigate vanishing gradients, techniques such as using activation functions that alleviate this issue, normalization methods like batch normalization, and gradient regularization strategies can be employed to encourage the flow of gradients during backpropagation. While these approaches help alleviate the vanishing gradient problem, they have not completely resolved it.

3.5. Applications of GANs to various tasks

GAN frameworks consist of two key components. The first is the generator, which explores underlying data structures and generates new images. This capability makes GANs particularly useful for addressing challenges like data scarcity and preserving patient privacy. The second component is the discriminator, which serves as a learned prior for normal images, enabling it to act as a regularizer or a detector for

abnormalities. The following subsections briefly outline some of the key applications of GANs.

3.5.1. Image reconstruction

Image reconstruction is the process of generating high-quality images from incomplete or low-quality data using algorithms or models. It is commonly used in fields such as medical imaging, computer vision, and remote sensing. In medical imaging, the objective is to create clear, high-quality images from blurry, low-resolution, or noisy inputs. For example, reconstructing clear, high-fidelity images from under-sampled MRI version. However, this process is inherently challenging due to its ill-posed nature. Deep learning generative models—in particularly GANs—are effective tools for improving image quality, including applications such as denoising, super-resolution, and improving medical scans, where clear and detailed images are essential for accurate diagnosis and analysis [77]. These data-driven deep learning methods either map raw sensory data inputs directly into output images or serve as post-processing techniques to improve image quality by addressing challenges such as noise, motion blur, missing information, or eliminating artifacts that compromise image quality. A GAN consists of two main components: a generator, which learns to create realistic images from random noise or imperfect data, and a discriminator, which assesses their quality. This approach has shown significant potential in advancing image reconstruction. Medical image reconstruction can be divided into two categories: image enhancement and image restoration.

- **Image Enhancement:** This focuses on improving the quality of existing images. For example, in low dose computed tomography (LDCT), reducing X-ray doses minimizes patient radiation exposure but often results in lower image quality. Enhancement algorithms are then needed to improve these images for accurate diagnostics [77].

- **Image Restoration:** This involves converting raw data into interpretable images for diagnosis and treatment planning. Recent advancements in the field of deep learning generative models—particularly GANs and diffusion models—have demonstrated substantial potential in advancing image reconstruction tasks, such as under-sampled MRI reconstruction, sparse view CT image reconstruction, and endoscopic video restoration. These models have shown significant potential to improve the accuracy and performance of image reconstruction systems [77].

3.5.2. Image synthesis

Medical image synthesis involves generating artificial or synthetic images that closely resemble real-world images. This technique is particularly valuable in healthcare settings where data scarcity and patient confidentiality present significant challenges. This technique enables the generation of diverse, privacy-compliant datasets for training robust machine learning models. Recent advancements in deep learning, particularly GANs, have shown great potential in addressing privacy concerns and overcoming the scarcity of rare pathology cases. Unlike traditional data augmentation methods, such as scaling or flipping, GANs are better suited to capture variations in imaging protocols and pathological features. GANs provide flexible solutions for tasks such as anomaly detection, data synthesis, and simulating medical conditions. This approach reduces imaging time and costs and generates training samples that maintain high anatomical accuracy.

3.5.3. Image detection

In medical image analysis, object detection involves identifying and localizing regions of interest (ROIs), like lung nodules in X-rays, which is crucial for diagnosis. However, it is time-consuming for clinicians, creating a need for accurate computer-aided diagnosis (CAD) systems to act as a second observer to speed up the process. GANs are highly effective in detection tasks within medical imaging. The GAN's discriminator can be utilized to detect abnormalities, like lesions, by learning the probability distribution of normal images. If a medical

image deviates from this distribution, it is flagged as abnormal. GANs can identify conditions such as cancer, tumors, anomalies, pneumonia, etc., by comparing synthetic healthy tissue images with real ones. The object detection approach can improve the accuracy of early disease detection, minimizing missed diagnoses and enhancing patient outcomes [78].

3.5.4. Image classification

Classification is one of the most successful applications of deep learning. In medical imaging, precise classification is critical for supporting clinical care and treatment decisions. Deep neural network, trained with class labels for individual images, are capable of extracting hierarchical features to make accurate classifications. For example, diagnosing malignant tumors at an early stage is essential for planning effective treatments and significantly increasing survival rates. Tumors can be either benign (non-cancerous) or malignant (cancerous) and identifying them accurately is vital. GANs have also been applied to classification tasks, either by using parts of the generator and discriminator as feature extractors or by employing the discriminator directly as a classifier, with an additional class for generated images. GANs enhance image classification by augmenting training data, improving domain alignment for robustness, refining image quality for better feature extraction, identifying anomalies, and providing unlabeled data for semi-supervised learning. This results in improved classifier accuracy and greater adaptability in a variety of use cases [79].

3.5.5. Image segmentation

Medical image segmentation plays a critical role in enhancing the visibility of anatomical or pathological changes within images. By segmenting key structures or objects in medical images and extracting relevant features from the segmented regions, this process significantly improves diagnostic efficiency and accuracy, aiding clinicians in making precise diagnoses. Earlier methods for medical image segmentation relied on techniques such as edge detection, active contours, statistical shape models, template matching, and machine learning, among others. Accurate segmentation remains essential for applications in computer-aided diagnosis, treatment planning, and image-guided surgery. GANs have demonstrated considerable potential in advancing segmentation tasks and have emerged as powerful tools in segmenting organs like lungs or managing scattered backgrounds in ultrasound scans [80]. These methods help reduce misclassification by capturing relationships between distant pixels, making them especially well-suited for segmenting large and complex organs.

3.5.6. Image registration

Image registration in medical imaging refers to the process of aligning multiple images of the same subject or structure, which may be captured at different time points or using different imaging modalities, to ensure spatial consistency and accurate correspondence. GANs are applied to enhance image registration by generating synthetic images that aid in the alignment process, thus improving accuracy in complex cases [81]. For example, Conditional GANs (cGANs) are used for both multimodal and unimodal image registration. In these scenarios, the generator either produces transformation parameters or directly generates the transformed image, while the discriminator differentiates between aligned and unaligned image pairs. Tanner et al. utilized CycleGAN for deformable image registration between MR and CT images [82]. The authors findings demonstrated that this method could achieve comparable performance to traditional multi-modal deformable registration techniques. Image registration plays a key role in tracking disease progression and evaluating treatment effectiveness. In image-guided procedures and radiation therapy, precise registration ensures accurate targeting and minimizes damage to surrounding healthy tissue.

3.5.7. Image segmentation

Image augmentation is commonly used in data and image processing, especially within the field of medical image analysis. In medical imaging, where datasets may be limited and diverse clinical cases are essential, augmentation plays a vital role in bridging this gap. By generating new training samples or modifying existing ones, augmentation enhances the robustness and generalization of machine learning models. One of the key technologies driving progress in this area is GANs, which have gained significant attention for their exceptional image generation capabilities. The basic augmentation methods can only generate a limited amount of data, and relying heavily on the original dataset, deep learning approaches—especially GANs—are capable of producing a broader range of data diversity, independent of the original dataset [83]. This capacity for generating rich and varied data enables more accurate training of models for disease detection, classification, and analysis of medical images. In areas where comprehensive and varied datasets are essential for producing reliable results and ensuring strong model performance, augmentation techniques significantly improve the quality and effectiveness of medical image analysis [84].

4. Methodology

A systematic literature review was conducted following the method outlined by Oates [64], focusing on publications related to “GANs” and their application in “medical image reconstruction.” The search utilized the following keywords: “generative adversarial networks” or “generative adversarial network,” “medical image” or “medical imaging,” and “image reconstruction.” The review included literature materials available in the ACM Digital Library up to August 31, 2023. The PRISMA flow diagram [65] was employed to ensure a clear and transparent reporting of the search process. Fig. 2 displays a customized PRISMA flow diagram that visually represents the search process and outlines the inclusion and exclusion criteria used to determine the eligibility of papers for the review. To address the data requirements, the primary research question aimed to explore the prevalence of GANs in medical image reconstruction over a specified period. To fulfill the data generation requirements, a document survey methodology was employed to collect relevant data from existing academic literature. Journal articles and conference proceedings related to GANs, and image reconstruction were selected based on established criteria to ensure the inclusion of credible and pertinent sources.

A total of 452 records were compiled from the ACM Digital Library to form the sampling frame. To refine the dataset, a systematic sampling technique was applied, resulting in 82 relevant articles for further analysis (see PRISMA flow diagram, Fig. 2, for details). The process comprises four phases: identification, screening, eligibility, and inclusion. To save space, the screening, eligibility, and inclusion phases are grouped together in the same row. In the identification phase, articles were sourced from the relevant databases. During the screening phase, inclusion and exclusion criteria were applied to these articles. In the eligibility phase, articles were evaluated for relevance, with those deemed ineligible excluded. Finally, the inclusion phase involved a thorough examination of the selected articles that met all criteria for inclusion in the study.

5. Results and discussion

In recent years, GANs have emerged as valuable tools for a diverse range of intricate tasks in medical image processing, particularly in the context of reconstructing medical images for different organs across various modalities. GANs appear to have demonstrated effectiveness in enhancing the quality of medical images by generating high-quality versions from lower-quality or incomplete source images.

One example that showcases this potential is from Zhang and colleagues, who introduced a 3D end-to-end generative adversarial

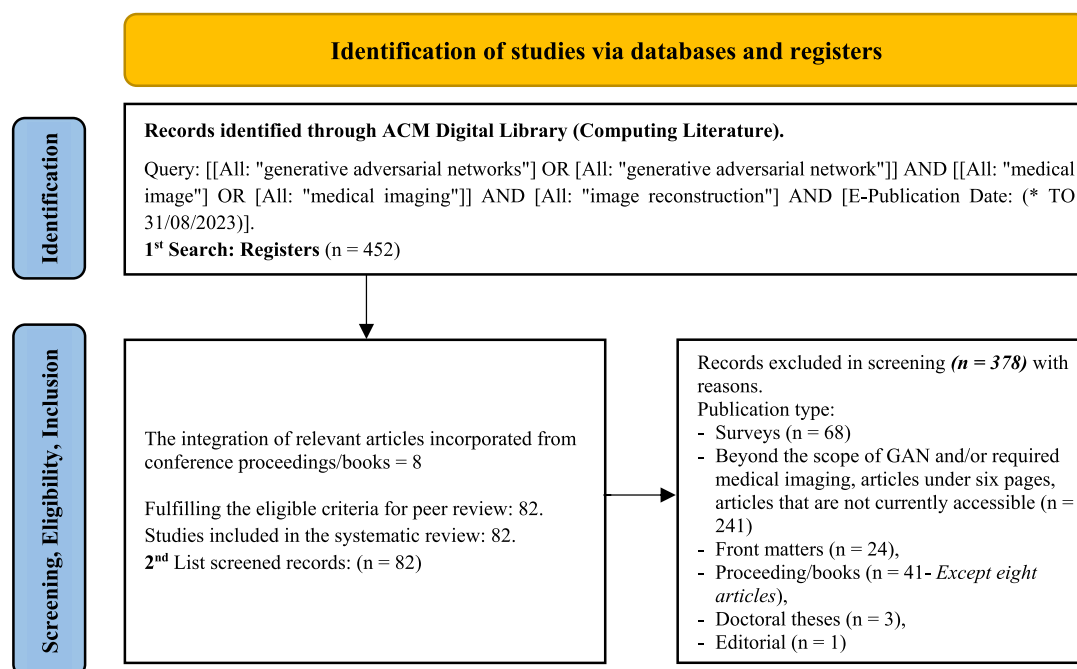


Fig. 2. A custom visual PRISMA flow diagram representation of the search process.

network called BPGAN [66]. This network can generate PET images from MRI scans, serving as a data completion method in multimodal medical imaging research. The authors assessed the BPGAN model using three quantitative evaluation metrics—namely, structural similarity index (SSIM), peak signal-to-noise ratio (PSNR), and the mean absolute error (MAE)—and demonstrated that it could successfully synthesize high-quality PET scans based on evaluation by those metrics. The authors collaborated with two clinical experts to visually analyze qualitative results, concluding that BPGAN-generated PET scans closely resemble ground truth data. The authors claimed that BPGAN excels in both qualitative and quantitative evaluations, effectively producing diverse and high-quality PET scans from MRI inputs. These generated PET scans add value when classifying Alzheimer's disease, even when dealing with missing data in the classification process.

In another study, Wang, and Zheng proposed an algorithm utilizing a conditional generative adversarial network to delineate areas of lung lesions caused by COVID-19 in CT images [67]. The authors demonstrated that the experimental results, which encompassed metrics such as ROC, F1-Score, and the Dice similarity coefficient, provided significant evidence for the accuracy and robustness of the proposed algorithm. The authors suggested that the proposed model has the potential to serve as a cost-effective and time-efficient medical tool for clinical diagnosis, offering significant support for computer-aided diagnosis.

In another study, Qiu and colleagues introduced an enhanced generative adversarial network (IGAN) algorithm for retinal image super-resolution reconstruction [68]. The model produced images with rich texture details and improved visual quality. The authors claimed that the IGAN approach demonstrated its effectiveness and reliability in analyzing retinal images, providing a solid basis for early clinical intervention.

Additionally, Molahasani and colleagues introduced an advanced and precise model named MSG-CapsGAN for enhancing the resolution of prostate MRI images [69]. The primary goal of this improvement was to facilitate early detection with the potential to save lives. The authors trained MSG-CapsGAN using the Prostate-Diagnosis and PROSTATEx datasets, illustrating MSG-CapsGAN's outperformance of the leading prostate super-resolution models by a considerable margin in terms of key similarity metrics, including PSNR, SSIM, and the multi-scale structural similarity index metric (MS-SSIM). In direct comparison

with other related techniques, MSG-CapsGAN, which had been specially designed for the identification of severe cancer cases, was shown to surpass these techniques in high-resolution super-resolution tasks.

Moreover, Wu and colleagues introduced an unsupervised approach for segmenting brain tumors, which they named the symmetric driven GAN (SD-GAN) [70]. This model was trained to understand the nonlinear relationship between left and right brain images, allowing it to capture the normal brain's symmetrical variations. The authors demonstrated that SD-GAN, an unsupervised approach, exhibited superior performance compared to other unsupervised segmentation techniques and showed competitive performance compared to supervised methods when tested on two public brain tumor datasets, BraTS2012 and BraTS2018.

In short, the studies discussed the significant advancements in medical imaging through the application of GANs. These developments hold promise for enhancing health-care diagnostics and early disease detection. The studies collectively emphasize the transformative impact of GAN-based approaches in enhancing medical imaging techniques for diverse clinical applications.

The ongoing systematic literature review revealed valuable and meaningful insights into the application of GANs across various dimensions, including task-based categorical distribution, organ-specific distribution, yearly trends, modality-wise distribution, and their role in image reconstruction for various organs and imaging modalities. Additionally, the review highlighted the utilization of datasets and evaluation metrics in the reviewed articles. The details are as follows.

5.1. Task-categorical distribution

The analysis presented in Fig. 3 illustrates the distribution of GAN-related research across diverse task categories, providing clear evidence of GAN's successful integration into numerous tasks within the medical domain. Notably, GANs have been frequently utilized for image enhancement and reconstruction tasks, with each type of task appearing in at least 33 articles. Additionally, GANs have been utilized in other tasks, including image/data generation, segmentation, transformation, augmentation, classification, and fusion, appearing in at least 10 articles for each category. Tasks other than reconstruction were not included in the search keywords. However, some studies addressed additional tasks

Task categorical distribution of GAN-related papers

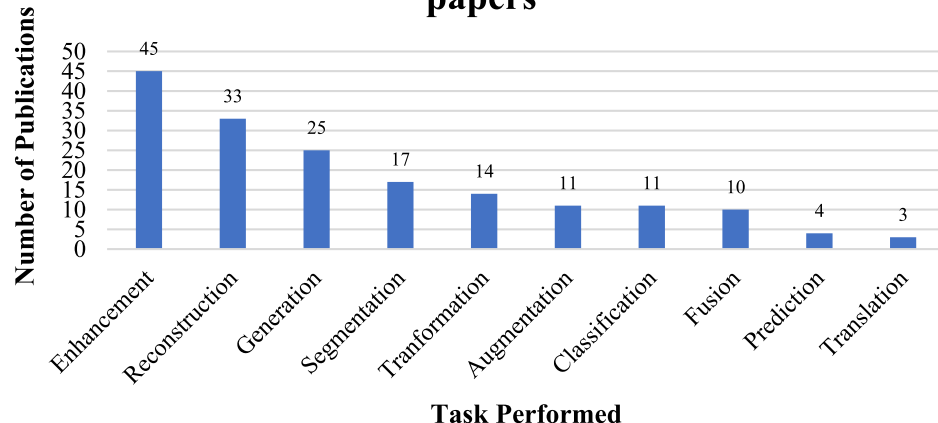


Fig. 3. Task-based categorical distribution of GAN related articles.

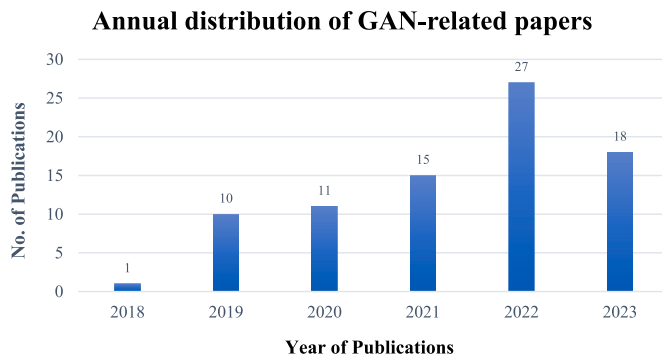


Fig. 4. Annual distribution of articles/papers on GANs.

simultaneously, leading to a form of leakage into this survey. This implies that either tasks other than image reconstruction were present within the subjects identified or a GAN had carried out these tasks as subtasks alongside the primary image reconstruction task. This highlights the versatility and effectiveness of GANs in addressing complex and diverse challenges in the field of medical imaging. It has been observed that there were instances where GANs were utilized for multiple tasks within a single article. Further details are provided in Appendix C.

5.2. Annual distribution

The analysis presented in Fig. 4 sheds light on annual research trends, highlighting a significant increase in the integration of GANs in

the medical sector. It provides an overview of GAN-related publications each year for diverse medical image processing tasks across different image modalities and organs. The analysis encompasses the period from the first publication in 2018 until August 31, 2023, including a total of 82 articles that met the selection criteria. For each year from 2019 to 2022, the annual publication figures stood at 10, 11, 15, and 27, respectively. As of August 2023, an additional 18 articles were published, indicating a consistent growth in GAN-related research in the field of medical image processing. This trend emphasizes the significant role of GANs in the evolving landscape of medical image analysis.

5.3. Organ-specific distribution

The analysis presented in Table 2 provides a detailed exploration of GAN applications at an organ-specific level, revealing a diverse range of uses in the medical field. These include but are not limited to disease diagnosis and the detection of anomalies such as lesions, cells, and nodules across anatomical regions such as the brain, eyes, blood, breast, chest/lungs, abdomen, heart, and knee. Notably, GANs have been frequently employed in image processing tasks related to brain and chest/lung organ images, with 33 articles dedicated to brain-related tasks and 20 focusing on chest/lung image processing. Additionally, GANs have been utilized for image processing tasks associated with different organs and body parts, including the eyes, abdomen, breast, knee bones, blood vessels, heart, liver, bones, and skin, with at least three articles dedicated to each organ or body part. These applications extend to disease diagnosis, where GANs play an important role in identifying conditions such as cancer and various abnormalities. See Appendix C for more details.

Table 2
Distribution of GAN-related papers across different organs.

Organ/Body parts	Number of Articles Covered	Organ/Body parts	Number of Articles Covered	Organ/Body parts	Number of Articles Covered
Brain	33	Head	2	Ligaments	1
Chest/Lungs	20	Musculoskeletal	2	Lower Limb bone	1
Eye	9	Ankle bone	1	Mediastinum	1
Abdomen	7	Artery	1	Pancreas	1
Breast	5	Backbone	1	Prostate	1
Knee bone	5	Blood	1	Stomach	1
Blood vessel	4	Bone cartilage	1	Tendons	1
Heart	4	Bone marrow	1	Throat-Nose back link	1
Liver	4	Cell (biological)	1	Tongue	1
Bone	3	Legs	1	Tooth	1
Skin	3	Note: GANs used for multiple organs in single articles observed frequently			

Modality	Number of Articles Covered	Modality	Number of Articles Covered
CT - Computed Tomography	35	SPECT - Single-Photon Emission Tomography	2
MRI - Magnetic Resonance Imaging	35	EM - Electron Microscopy	1
PET - Positron Emission Tomography	11	Endoscopy	1
Conventional Radiography - X-ray	10	FM - Fluorescence Microscopy	1
RF - Retina Fundus/OCT - Optical coherence tomography/DR Diabetic Retinopathy	8	GC - Grayscale Characters	1
RGB - Red Green Blue	4	KI/PI - KI Images/Parametric Images	1
US - Ultrasound	4	MO - Microscopic Organisms Images	1
DL - Dermoscopic Lesion Images	2	PACT - Photoacoustic Computed Tomography	1
Singogram	2	PNG - Portable Network Graphic	1

5.4. Modality-wise distribution

The analysis presented in Table 3 reveals the widespread application of GANs across a diverse spectrum of modalities, emphasizing their flexibility and adaptability. Beyond traditional imaging methods such as X-ray, CT, MRI, US, and retinal fundus (RF) and red, green, and blue (RGB) imaging, GANs have found applications in techniques such as PET, showcasing their transformative impact on different diagnostic methodologies. Within the medical domain, the research distribution highlights varying areas of emphasis among different modalities. Notably, 35 of the research papers reviewed focused on CT, while the same number centered on MRI. About 11 of the documents focused on PET, while 10 were dedicated to X-ray. On the other hand, RF, OCT, and DR collectively accounted for eight of the research papers reviewed. US and RGB imaging were each covered in four papers. Additionally, two papers focused on each of DL, sinograms, and SPECT. Furthermore, EM, endoscopy, FM, GC, KI/PI, MO, PACT, and PNG collectively comprised eight of the research papers reviewed. It has been noted that GANs are frequently employed for multiple modalities in individual subjects (See Appendix C for more details). Together, these research efforts highlight the significant contribution of GANs in the realm of medical image analysis. Their incorporation into various radiological and non-radiological modalities underscores their broad participation in the medical sector. The varying proportions of GAN-related research dedicated to specific modalities emphasizes the multifaceted role of GANs in medical imaging.

5.5. GANs in image reconstruction

Table 4 highlights the diverse applications of GANs in image reconstruction across various organs and imaging modalities, showcasing their adaptability and importance in the medical field. GANs are most frequently used for brain image reconstruction (15 studies), followed by chest/lung (8 studies), and eye and knee (4 studies each). Additionally, GANs have been applied to reconstruct images of other organs, such as the abdomen, breast, heart, liver, bones, and skin, with at least one study addressing each.

Regarding imaging modalities, GANs have been most commonly used for MRI and CT data reconstruction, with 15 and 13 studies, respectively. This is followed by 6 studies focused on PET data and 3 studies on X-ray data reconstruction. The reconstruction of retina fundus (RF), optical coherence tomography (OCT), and diabetic retinopathy (DR) data has been explored collectively in 3 studies. Furthermore, ultrasound, and sinogram data reconstruction have been investigated in 2 studies, while SPECT, RGB, and PACT data reconstruction were investigated in at least one study each.

The studies indicate that various types of GANs have been utilized for image reconstruction task across different organs using various imaging modalities to meet specific application needs. For instance, Task-GAN [85], Semi-supervised GAN [86], Knowledge Infusion (Ki-GAN) [87], Multi-modal Fusion (MMFGAN) [88], Medical Image Super-resolution (MedSRGAN) [89], Improved GAN (IGAN) [90], Progressive Wasserstein GAN (PWGAN-WGAN) [91] with a weighted structurally-sensitive hybrid loss function, Dual-domain GAN [92], Reconstruction Global-Local GAN (Recon-GLGAN) [93], Parallel Imaging Coupled Dual Discriminator GAN (PIDD-GAN) [94], Lightweight GAN [95], Multi-task Discriminator GAN (MTD-GAN) [96], Swin Transformer GAN (SwinGAN) [97], 3D-MedTranCSGAN [98], Conditional GAN (cGAN) [99], 3D Transformer-GAN [100], Symmetric Driven GAN (SD-GAN) [101], GAN-based frameworks for fast MRI reconstruction [102], cGAN-based Blind Image Denoising Network (NR-BIDN) [103], Super-resolution Attention GAN (SAGAN) [104], 3D cGAN-based Intelligent Parallel Distributed Streaming Framework (IPDSF) [105], Attention Denoising Super Resolution GAN (AID-SRGAN) [106], PatchGAN-based networks (P-Net) [107], Perceptual Supervised GAN methods [108], and Wasserstein GAN with Gradient Penalty (WGAN-GP) [109].

Table 4

GAN usage frequency in image reconstruction across various organs and imaging modalities.

GAN application frequency in image reconstruction across different organs and modalities			
Organ	GAN usage frequency	Modality	GAN usage frequency
Brain	15	MRI	15
Chest/Lungs	8	CT	13
Eye	4	PET	6
Knee bone	4	X-ray	3
Abdomen	2	RF, OCT, DR	3
Heart	2	US	2
Blood	2	Sinogram	2
Breast	1	RGB	1
Blood vessel	1	SPECT	1
Liver	1	PACT-Photoacoustic CT	1
Bone	1	Abbreviation:	
MSK - Musculoskeletal	1	RF-Retina Fundus	
Ankle bone	1	OCT-Optical coherence tomography	
Lower Limb bone	1	DR-diabetic retinopathy	

Table 5

Overview of datasets used in GAN applications across the reviewed papers/articles.

Reviewed Articles and Datasets	Quantity
Number of papers/articles using publicly accessible datasets	42
Number of papers/articles using private datasets	23
Number of papers/articles utilizing both public and private datasets	17
Total articles reviewed	82
Datasets (Public and Private)	Quantity
Number of public datasets in total	85
Total public dataset usage count	117
Number of private datasets in total	37
Total public dataset usage count	58
Total count of datasets (public and private)	122
Total count of dataset usage (public and private)	175

See [Appendix D](#) for more details.

These research efforts collectively highlight the significant role of GANs in image reconstruction task. The application of GANs across various organs under different imaging modalities—both radiological and non-radiological—underscores their widespread involvement in enhancing image reconstruction. This underscores the diverse and essential contribution of GANs to the advancement of medical imaging.

Table 6

Overview of private datasets used in GAN-based research.

Sr. #	Private Datasets	Usage Frequency	Sr. #	Private Datasets	Usage Frequency
1	Synthetic and/or Private dataset	19	20	Hamamatsu SHR22000 (Brain PET data)	1
2	Clinical dataset	2	21	Hoffman brain datasets (Monte Carlo simulation data)	1
3	In-vivo dataset	2	22	iSee - Fundus Multi-disease Diagnosis dataset	1
4	MDME - Multi-Dynamic Multi-Echo Acquisition	2	23	Knee Bones dataset	1
5	Abdominal dataset	1	24	L-CT-A dataset	1
6	Ankle bones dataset	1	25	L-CT-G dataset	1
7	Augmented dataset	1	26	LC sinogram (Combination of AnsysFluent and GATE)	1
8	Breast ultrasonography images (Cls-Set, Rec-Set)	1	27	Lower Limb Bones dataset	1
9	CBMFM - Chinese Brain Molecular and Functional Mapping	1	28	Medical dataset - Liver CT image medical dataset	1
10	Clinical knee MR acquisitions dataset	1	29	MP2RAGE (Magnetization Prepared 2 Rapid Acquisition Gradient Echoes) sequences dataset	1
11	CTA - CT Angiography dataset	1	30	MPRAGE (Magnetization-Prepared Rapid Gradient-Echo) sequences dataset	1
12	CTP - CT Perfusion dataset	1	31	Bone Marrow Microscopic Image dataset	1
13	Dataset D1- (NCCTs-Non-contrast & CECT images)	1	32	PE-CT dataset	1
14	Dataset D2- (NCCTs-Non-contrast & CECT images)	1	33	RSD - Rail Surface Defect dataset	1
15	Dataset D3(CECT-Contrast-Enhanced CT and VNCCT-Virtual Non-Contrast CT Images)	1	34	TD - Tongue Data dataset	1
16	DIR (Double Inversion Recovery) sequences	1	35	UCHCDM - University of Connecticut Center DigiMammo database	1
17	FLAIR (Fluid-Attenuated Inversion Recovery) sequences	1	36	Zubal Brain dataset (Monte Carlo simulation data)	1
18	FRD - Fundus Retinal Dataset	1	37	Zubal Thorax datasets (Monte Carlo simulation data)	1
19	Full-Sampled Data	1			

5.6. Overview of the datasets

The analysis in [Table 5](#) provides a comprehensive overview of the datasets employed in GAN applications within the scrutinized articles. The study involved 82 articles, with 42 exclusively incorporating one or more publicly available dataset and 23 relying solely on one or more private datasets. Notably, 17 articles judiciously leveraged both public

Table 7

Overview of top public datasets used in GAN-based research.

Sr. #	Public Datasets	Usage Frequency	Sr. #	Public Datasets	Usage Frequency
1	BraTS2018 - Brain Tumor Segmentation Challenge	4	44	EyeQ - Eye-Quality Assessment	1
2	IXI - eXtraction from Images	4	45	FFHQ - Flickr-Faces-HQ	1
3	ANDI - Advanced Neuropsychological Diagnostics Infrastructure	3	46	FIRE - Fundus Image Registration	1
4	BraTS2020 - Brain Tumor Segmentation Challenge	3	47	FSE knee	1
5	DIV2K	3	48	HCP	1
6	LUNA16 - LUNG Nodule Analysis	3	49	HRF	1
7	Mayo Clinic Low Dose CT Grand-2016 NIH Challenge	3	50	IDRiD	1
8	MICCAI	3	51	Image dataset of the overhead catenary system of the high-speed train (Southwest Jiaotong University (ed) 2012)	1
9	ACDC - Automated Cardiac Diagnosis Challenge	2	52	Image Fusion	1
10	Brainweb MRI	2	53	IOSTAR	1
11	BraTS2019 - Brain Tumor Segmentation Challenge	2	54	ISBI2009	1
12	ChestX-ray14	2	55	ISBI2012	1
13	CIFAR10	2	56	ISBI2014	1
14	DRIVE	2	57	PH2	1
15	EyePACS - Eye Picture Archive Communication System	2	58	ISLES2015 - Ischemic stroke lesion segmentation challenge	1
16	FASTMRI	2	59	Kaggle	1
17	ISIC 2016/18	2	60	LoDoPab-CT	1
18	JSRT - Japanese Society of Radiological Technology	2	61	Medical Segmentation Decathlon (brain tumors)	1
19	LIDC-IDRI	2	62	MNIST	1
20	Messidor	2	63	MRNet knee	1
21	Set14	2	64	MR-T1/PET - Harvard Medical School	1
22	Set5	2	65	MR-T1/MR-T2 - Harvard Medical School	1
23	102-Flowers	1	66	MURA - Musculoskeletal RAdiographs	1
24	AANLIB	1	67	Neoplastic Disease (brain tumor) from AANLIB	1
25	AAPM - American Association of Physicists in Medicine	1	68	NPC - Nasopharyngeal Carcinoma	1
26	AIBL - Australian Imaging, Biomarker & Lifestyle	1	69	OASIS - Open Access Series of Imaging Studies	1
27	ALL-IDB1 - Acute lymphoblastic leukaemia-international database	1	70	Partial-CelebA	1
28	BraTS2012 - Brain Tumor Segmentation Challenge	1	71	Periapical Radiographic Images	1
29	BraTS2015 - Brain Tumor Segmentation Challenge	1	72	Pneumonia Chest X-ray dataset of Kaggle platform	1
30	BraTS2021 - Brain Tumor Segmentation Challenge	1	73	Prostate-Diagnosis	1
31	BreastMNIST	1	74	PROSTATEx	1
32	BSD100	1	75	QIN - Quantitative Imaging Network (Breast dataset)	1
33	BTD - Brain Tumor Detection	1	76	RAISE	1
34	Calgary-Campinas Public Brain MR	1	77	RESC - Retinal Edema Segmentation Challenge	1
35	CCA-US - Common Carotid Artery Ultrasound	1	78	SK110 - Segmentation of Knee Images 2010	1
36	CHASEDB1	1	79	SLIVER07-Segmentation of the Liver Competition 2007	1
37	CORD-19 - COVID-19 Open Research Dataset Challenge	1	80	SN-AM dataset (White Blood Cancer Dataset of B-ALL and MM for Stain Normalization)	1
38	COVID-19 CT Segmentation	1	81	STS - Soft-Tissue Sarcoma (PET-CT)	1
39	COVID-19_Dataset from the University of Montreal	1	82	TCIA - The Cancer Imaging Archive	1
40	COVID-Chest X-ray	1	83	Urban100	1
41	CVC-ClinicDB	1	84	US-CASE	1
2	DRHAGIS	1	85	Whole Brain Atlas database of Harvard Medical	1
43	DSB - Data Science Bowl 2017	1			

and private datasets in their investigative endeavors, aligning with the inherent dependence of GAN-based models' training on diverse and extensive training data. This strategic approach aimed to assess the model's generalizability, conducting rigorous verification, testing with real out-of-distribution datasets, and/or addressing overfitting concerns.

The analysis involved a total of 122 datasets, including both publicly accessible and private data sources. The cumulative count of dataset utilization reached 175, highlighting instances where multiple datasets had been employed within specific articles. Of the 122 datasets overall, 85 were public, contributing to an aggregate public dataset usage count of 117. In contrast, 37 datasets were private, with a total private dataset

usage count of 58. These datasets varied in size and served as inputs to various GAN network architectures employing different loss functions, substantially influencing GAN performance. Additional detail of the datasets is provided in [Appendix A](#).

The analysis in [Table 6](#) delineates private datasets (37 of 122) employed in GAN-related research in the papers/articles scrutinized. Unnamed private datasets, consisting of 19 out of 37, were classified as "synthetic and/or private datasets" alongside approximately 18 explicitly named private datasets. This implies that these private datasets were not publicly available when the associated papers were published. Notably, the private datasets, specifically identified as {Clinical dataset,

Table 8

Top metrics for assessing GAN-based methods in medical image processing.

Sr. #	Metrics	Usage Frequency	Sr. #	Metrics	Usage Frequency
1	SSIM - Structural Similarity Index	56	46	Blum - Chen-Blum Indicator	1
2	PSNR - Peak Signal-to-Noise Ratio	51	47	CE - Cross Entropy	1
3	Sensitivity/Recall	19	48	CI - Contrast Index	1
4	DSC or DICE - Dice Similarity Coefficient	15	49	Conformity	1
5	Accuracy	12	50	Correlation	1
6	Precision	11	51	Energy	1
7	AUC - Area Under the ROC Curve	9	52	F - Measure	1
8	FID - Fréchet inception distance	8	53	FMI - Feature Mutual Information	1
9	JI-Jaccard Index or IoU-Intersection over Union	7	54	FNR - False Negative Rate	1
10	Specificity	7	55	FPS - Frame Per Second	1
11	MSE - Mean Square Error	6	56	GMSD - Gradient Magnitude Similarity Mean	1
12	RMSE - Root Mean Squared Error	6	57	Homogeneity	1
13	NMSE - Normalized Mean Square Error	5	58	IFC - Information Fidelity Criterion	1
14	Params - (Number of Parameters)	5	59	Informedness	1
15	VIF - Visual Fidelity	5	60	Intensity	1
16	EN - Entropy	4	61	IS - Inception Score	1
17	HD - Hausdorff Distance	4	62	JND - Just Noticeable Distortion	1
18	MAE - Mean Absolute Error	4	63	Kappa	1
19	ROC - Receiver Operating Characteristic	4	64	L1 (Least Absolute Deviations) Loss	1
20	Time	4	65	Laplace Variance	1
21	F1-Score	3	66	Markedness	1
22	MI - Mutual Information	3	67	MMD - Maximum Mean Discrepancy	1
23	MOS - Mean Opinion Score	3	68	MS-SSIM - Multi-Scale Structural Similarity Index Metric	1
24	SD - Standard Deviation (noise)	3	69	MSD - Mean Surface Distance	1
25	AG - Average Gradient	2	70	NCC - Normalized Cross Correlation	1
26	BRISQUE Score	2	71	NCIE - Nonlinear Correlation Information Entropy	1
27	FPR - False Positive Rate	2	72	NIQE - Natural Image Quality Evaluator	1
28	FSIM - Feature Similarity Index Measurement	2	73	NMAE - Normalized Mean Absolute Error	1
29	Likert Score	2	74	PIQE-Perception based Image Quality Evaluator	1
30	LPIPS-Learned Perceptual Image Patch Similarity	2	75	PL - Perceptual Loss	1
31	MCC - Matthew's Correlation Coefficient	2	76	Positive and Negative Predictive Value	1
32	Mean	2	77	QFAB - Fusion from A to F	1
33	NRMSE -Normalized Root Mean Square Error	2	78	Recon Time	1
34	Qabf - Gradient-Based Fusion Performance	2	79	Reproducibility	1
35	ROI - Region of Interest	2	80	RVD - Relative Volume Difference	1
36	SF - Spatial Frequency	2	81	SND - Standard Normal Distribution	1
37	t-test	2	82	SNR - Signal - to - Noise Ratio	1
38	TPR - True Positive Rate	2	83	TML - Texture Matching Loss	1
39	UQ - Universal Image Quality Index	2	84	TPR - True Negative Rate	1
40	Visual Turing Test	2	85	TSSA - Task-Specific Similarity Assessment	1
41	Wilcoxon Paired Test	2	86	Variance	1
42	AQE - Automatic Quality Evaluation	1	87	VD - Volume Difference	1
43	ASSD - Average Symmetric Surface Distance	1	88	VOE - Voxel Overlap Error	1
44	BCE - Binary Cross Entropy (Loss)	1	89	Wavelet	1
45	Bias	1			

Table 9

Summary of datasets, metrics, objectives, organs, and modalities.

Summary of the datasets, metrics, tasks, organs, and modalities	
Category/Entity	Quantity
Number of datasets in total (public and private)	122
Total dataset usage count (public and private)	175
Number of metrics in total	89
Total metrics usage count	335
Number of tasks in total	10
Count of total tasks performed	173
Number of organs served in total	31
Total organ servings count	119
Number of modalities served in total	18
Count of modalities servings in total	121

MDME, and In-vivo datasets}, coincidentally shared identical names, reflecting their acquisition through similar private technologies. Each of these datasets was employed in two articles. Further details can be found in [Appendix A](#).

The analysis in [Table 7](#) highlights the top publicly available datasets (85 out of 122) employed in GAN-related research in the scrutinized papers/articles. The datasets, identified as {BraTS2018, IXI, ANDI, BraTS2020, DIV2K, LUNA16, Mayo Clinic Low Dose-CT Grand-2016 NIH Challenge, and MICCAI}, sourced from publicly accessible repositories, were employed in a minimum of three articles each. In the subsequent tier, datasets identified as {ACDC, Brainweb MRI, BraTS2019, ChestX-ray14, CIFAR10, DRIVE, EyePACS, FASTMRI, ISIC, J2018/JPLISPH-2018 IDRI, Messidor, Set14, and Set5}, sourced from publicly accessible repositories, were employed in a minimum of two articles each. The remaining datasets were employed individually, each appearing in a single article. See [Appendix A](#) for more details.

5.7. Overview of evaluation metrics

The analysis in [Table 8](#) portrays the evaluation metrics employed for assessing the approaches within the reviewed articles. Among these metrics, the structural similarity index - SSIM [71–73] and peak signal-to-noise ratio – PSNR [71,74] stand out as the most utilized, appearing in 56 and 51 articles/papers, respectively. Following these, sensitivity/recall, the Dice coefficient, and accuracy are noteworthy as the next most utilized metrics, appearing in 19, 15, and 12 articles/papers, respectively. Further details can be found in [Appendix B](#).

The SSIM is used in image processing and computer vision to quantify the structural similarity and perceptual quality of two images. It measures the visual quality of an image by considering aspects such as luminance, contrast, and structure [73]. The SSIM is calculated using the formula in equation (4) [73]:

$$\text{SSIM}(\mathbf{x}, \mathbf{y}) = l(\mathbf{x}, \mathbf{y})^\alpha \cdot c(\mathbf{x}, \mathbf{y})^\beta \cdot s(\mathbf{x}, \mathbf{y})^\gamma, \quad (4)$$

where $\text{SSIM}(\mathbf{x}, \mathbf{y})$ is the SSIM index between two images, \mathbf{x} and \mathbf{y} ; $l(\mathbf{x}, \mathbf{y})$ represents the luminance comparison; $c(\mathbf{x}, \mathbf{y})$ represents the contrast comparison; and $s(\mathbf{x}, \mathbf{y})$ represents the structure comparison. Setting the weights α , β , and γ to 1 simplifies the formula, as shown in equation (5):

$$\text{SSIM}(\mathbf{x}, \mathbf{y}) = l(\mathbf{x}, \mathbf{y}) \cdot c(\mathbf{x}, \mathbf{y}) \cdot s(\mathbf{x}, \mathbf{y}), \quad (5)$$

The PSNR is also a commonly used image quality metric found in various domains, including medical image processing [74]. Its primary

purpose is to assess image quality by comparing a processed or reconstructed image to a reference or original image. PSNR can be applied to assess the quality of medical images such as X-rays, MRIs, CT scans, and US images. The PSNR is calculated using the formula in equation (6) [74]:

$$\text{PSNR} = 20 \cdot \log_{10}(\mathbf{MAX}) - 10 \cdot \log_{10}(\mathbf{MSE}), \quad (6)$$

where \mathbf{MAX} is the maximum possible pixel value in an image (for 8-bit grayscale images, \mathbf{MAX} would typically be 255) and \mathbf{MSE} (mean squared error) is the average of the squared differences between corresponding pixels in the original image and the processed image. A higher PSNR value indicates that the processed image is more similar to the original.

In data science, models are often evaluated using precision and recall (sensitivity), while in the medical field, specificity and sensitivity are common metrics for assessing medical tests. These metrics (recall (sensitivity), precision, specificity) offer valuable insights into the model's performance. The expressions of these metrics are given below.

The Recall/Sensitivity/True Positive Rate (**TPR**) reflects the accuracy in identifying positive samples, calculated as the number of correctly predicted positive samples by the model (True positive - \mathbf{TP}) divided by the total number of designated/observed positive samples, as shown in equation (7) [75]:

$$\text{Recall} = \text{Sensitivity} = \frac{\mathbf{TP}}{\mathbf{TP} + \mathbf{FN}}, \quad (7)$$

where \mathbf{FN} represents false negatives: The positive samples classified as negative by the model.

The Specificity reflects the accuracy in identifying negative samples, calculated as the number of correctly predicted negative samples by the model (True negative - \mathbf{TN}) divided by the total number of designated/observed negative samples, as shown in equation (8) [75]:

$$\text{Specificity} = \frac{\mathbf{TN}}{\mathbf{TN} + \mathbf{FP}}, \quad (8)$$

where \mathbf{FP} represents false positives: negative samples classified as positive by the model.

Precision is the ratio of true positives to total number of predicted positives, meaning that precision is defined as the number of true positives (\mathbf{TP}) over the number of true positives plus the number of false positives (\mathbf{FP}), as shown in equation (9) [27]:

$$\text{Precision} = \frac{\mathbf{TP}}{\mathbf{TP} + \mathbf{FP}}, \quad (9)$$

The Dice coefficient [67], also known as the Dice similarity coefficient or the Sørensen–Dice coefficient, is a statistical metric used to measure the similarity or overlap between two sets or groups. It is commonly used in fields such as image segmentation, data analysis, and bioinformatics. The Dice coefficient is a valuable tool for assessing the accuracy and quality of image segmentation techniques, especially in medical imaging, computer vision, and remote sensing applications, among others. The formula for the Dice coefficient is shown in equation (10):

$$\text{Dice coefficient (DSC)} = \frac{2 \cdot |\mathbf{A} \cap \mathbf{B}|}{|\mathbf{A}| + |\mathbf{B}|}, \quad (10)$$

where \mathbf{A} represents the segmented region or objects obtained from the

algorithm being evaluated, \mathbf{B} represents the ground truth region or objects, $|\mathbf{A} \cap \mathbf{B}|$ is the size of the intersection of \mathbf{A} and \mathbf{B} (the number of pixels or voxels common to both the segmented and ground truth regions), $|\mathbf{A}|$ is the size of the segmented region \mathbf{A} , and $|\mathbf{B}|$ is the size of the ground truth region \mathbf{B} . The Dice coefficient yields a value in the range of $[0, 1]$, where “0” means no overlap between the segmented region and the ground truth, indicating poor segmentation, and “1” indicates perfect agreement between the two regions, indicating accurate segmentation. Table 8 provides an overview of 89 evaluation metrics utilized within this research review and their usage frequency in the evaluation of medical images.

5.8. Summary

The analysis in Table 9 portrays a comprehensive summary of the datasets, metrics, tasks, organs, and modalities analyzed within the articles reviewed. There were 122 top datasets in total, with a collective usage count of 175 throughout the articles. Furthermore, there were 89 top metrics, with a collective usage count of 335 throughout the articles. Additionally, the articles covered a total of 10 different tasks, with a combined task count of 173. In terms of organs, there were 31 distinct organs served throughout the articles, and these organs were the focus of 119 individual instances in the articles. Finally, the study identified 18 distinct modalities in the articles examined, with GANs applied in 121 instances across these modalities. Collectively, these research endeavors underscore the impact of GANs in the field of medical imaging. The diverse distribution of GAN-related research across numerous datasets, evaluation metrics, tasks, organs, and modalities underscore the versatile role of GANs in the field of medical imaging.

The aforementioned observations indicate that the utilization of GANs is significant and notable across various dimensions, encompassing task-categorical, organ-specific applications, annual trends, and their role in image reconstruction for various organs and imaging modalities, as well as their application in diverse radiological and non-radiological modalities. It can also be observed that the search keywords were limited to reconstruction task. However, it was found that GANs executed additional tasks, suggesting that these tasks were either intrinsic to the identified subjects or that GAN performed them as sub-tasks alongside the primary reconstruction task. These diverse tasks encompassed image/data generation, segmentation, transformation, augmentation, classification, fusion, prediction, enhancement, and translation.

Furthermore, the research revealed the capacity of GANs to excel in cross-modality tasks. As an example, the BPGAN model introduced by Zhang and colleagues [72] effectively generates high-quality PET scans from MRI inputs, facilitating the seamless conversion of images from one domain to another within the medical context. This demonstrates GAN's adaptability and potential in bridging gaps between different imaging modalities, thereby enriching the diagnostic process. The research also emphasizes GAN's role in image enhancement, which encompasses the synthesis, augmentation, and reconstruction of images. This underscores the capability of GANs to produce an extensive array of samples that bear significant resemblance to authentic ones. In doing so, GANs become instrumental in enhancing the quality and diversity of image datasets, thereby contributing to more effective model training. In the broader scope of model training, the integration of GANs into the process has proven to be highly beneficial.

Moreover, it was observed that a variety of GANs were employed in

both public and private datasets of varying sizes, utilizing a range of evaluation metrics to assess the effectiveness of the methods. Model training is intrinsically reliant on the availability of diverse, plentiful, and comprehensive training data to ensure a model's ability to generalize well on unseen test data while avoiding the pitfall of overfitting. These aspects reveal a direct correlation between network size and batch size during training. This underlines the significant role that a meticulously crafted network structure plays in achieving remarkable GAN performance. It is important to acknowledge, however, that although adjustments to GAN architecture can bring about improvements, they may not comprehensively address all the inherent training challenges associated with these models. Furthermore, refining the loss function through techniques such as normalization and regularization emerged as a valuable strategy in establishing more stable training results for GANs. By applying such methods, training outcomes can be rendered more consistent and dependable. The alterations introduced to the GAN architecture also resulted in improvements in training stability and a noticeable enhancement in the diversity and quality of the generated images. Collectively, these elements highlight the considerable impact and contribution of GANs in the realm of AI&ML in medical image processing.

GANs have found applications in various tasks beyond image reconstruction, including image/data generation, segmentation, transformation, detection, augmentation, classification, and fusion. Although tasks other than reconstruction were not explicitly included in the search keywords, some studies inadvertently addressed additional tasks, resulting in a form of leakage into this survey. This implies that either tasks beyond image reconstruction were covered in the identified subjects or GANs were employed to perform these tasks as subtasks alongside the primary image reconstruction task. This underscores the versatility and effectiveness of GANs in tackling complex and diverse challenges in medical imaging.

The analysis, confined to the ACM Digital Library databases, may not have been exhaustive, but it is expected that these studies will contribute sufficient knowledge, aiding both novice and experienced researchers in selecting research topics and refining methodological approaches within the studied subject.

6. Conclusion

The study has provided valuable insights into GAN-related research across various dimensions, including task-categorical distribution, organ-specific distribution, yearly trends, and applications in various modalities. It has concluded that 122 datasets were used in 175 instances, 89 metrics were employed 335 times, there were 10 different tasks with a total count of 173, 31 distinct organs featured in 119 instances, and 18 modalities were utilized in 121 instances across the reviewed articles, collectively depicting the significant utilization of GANs in medical imaging.

GANs have demonstrated versatility in tackling complex challenges, particularly in image enhancement and reconstruction tasks, as evidenced by at least 33 articles. Furthermore, GANs found applications in other tasks too, such as image/data generation, segmentation, transformation, augmentation, classification, and fusion, with a minimum of 10 articles for each category. However, the expansion of tasks (those not covered by the search keywords) beyond the intended reconstruction task reveals the potential for leakage into this survey, since some studies simultaneously addressed additional tasks alongside the primary image

reconstruction task, showcasing the adaptability and efficacy of GANs in diverse medical imaging challenges. Furthermore, the adaptability of GANs in cross-modality tasks demonstrates their potential to bridge gaps between different imaging modalities and to enrich the diagnostic process.

The study identified 82 research papers, of which 42 used public datasets and 23 used private datasets, and 17 articles utilized both public and private datasets. The private datasets consist of anonymized datasets categorized as “synthetic and/or private datasets,” along with named private datasets. This implies that only approximately half (42 out of 82 studies) can be reproduced, since the remaining 40 studies employed at least one private dataset.

GANs played a significant role in generating synthetic images/data, enhancing model training effectiveness by producing diverse samples closely resembling authentic images. The integration of GANs into model training highlights their substantial contribution to improving training stability. The intricate balance between network size, batch size, and loss function refinement, significantly influences GAN performance, though overcoming all associated training challenges remains a complex task. The continuous growth in GAN-related research, evident in annual trends, underscores the significant role of GANs in medical imaging. Collectively, these findings emphasize the importance and contribution of GANs in the field of AI&ML in medical imaging. This study demonstrates that GANs are effective tools in medical imaging, showcasing their potential to drive advancements in healthcare. In the future, GANs may significantly contribute to diagnosing diseases and detecting anomalies, particularly in identifying conditions such as cancer across different anatomical regions. The research serves to assist both novice and experienced researchers in directing their choice of research topics and the development of methodological approaches.

CRediT authorship contribution statement

Jabbar Hussain: Writing – review & editing, Writing – original draft, Visualization, Methodology, Formal analysis, Data curation, Conceptualization. **Magnus Båth:** Writing – review & editing, Supervision, Conceptualization. **Jonas Ivarsson:** Writing – review & editing, Validation, Supervision, Conceptualization.

Future directions

In the future, we suggest exploring additional open database sources with an extended cutoff date to validate our findings. Furthermore,

exploring the application of diffusion models in this field could be an important avenue for future research. Future research should also prioritize ethical considerations and the responsible use of AI&ML models.

Ethical and social consideration

In the context of this literature review, the consideration of ethical and social implications stemming from the findings was deemed unnecessary. It is anticipated that these results will not adversely impact people's lives in any manner.

Human and animal rights

The authors declare that the work described has been carried out in accordance with the [Declaration of Helsinki](#) of the World Medical Association revised in 2013 for experiments involving humans as well as in accordance with the EU Directive [2010/63/EU](#) for animal experiments.

The authors declare that the work described has not involved experimentation on humans or animals.

Informed consent and patient details

The authors declare that this report does not contain any [personal information](#) that could lead to the identification of the patient(s) and/or volunteers.

The authors declare that they obtained a written [informed consent](#) from the patients and/or volunteers included in the article and that this report does not contain any [personal information](#) that could lead to their identification.

The authors declare that the work described does not involve patients or volunteers.

Declaration of competing interest

The authors declare that they have no known competing financial interests or personal relationships that could have appeared to influence the work reported in this paper.

Acknowledgment

This work was supported by the Wallenberg AI, Autonomous Systems and Software Program - Humanity and Society (WASP-HS), funded by the Wallenberg Foundations, Sweden.

Appendix A

Appendix A. Presents a comprehensive overview of datasets (public and private) utilized in the scrutinized papers/articles

Appendix B

Appendix B. Provides a comprehensive overview of the evaluation metrics employed in the scrutinized papers/articles pertaining to medical image analysis

Appendix C

Appendix C. Provides a comprehensive an overview of GANs' use in various tasks across multiple organs and imaging modalities.

Appendix D

Appendix D. Provides an overview of GAN applications in image reconstruction across different organs and imaging modalities

References

- [1] J. Xia, Z. Wang, D. Yang, R. Li, G. Liang, H. Chen, A.A. Heidari, H. Turabieh, M. Mafarja, Z. Pan, Performance optimization of support vector machine with oppositional grasshopper optimization for acute appendicitis diagnosis, *Comput. Biol. Med.* 143 (2022) 105206.
- [2] J. Hu, A.A. Heidari, Y. Shou, H. Ye, L. Wang, X. Huang, H. Chen, Y. Chen, P. Wu, Detection of COVID-19 severity using blood gas analysis parameters and Harris hawks optimized extreme learning machine, *Comput. Biol. Med.* 142 (2022) 105166.
- [3] G. Litjens, T. Kooi, B.E. Bejnordi, A.A.A. Setio, F. Ciompi, M. Ghafoorian, J.A. Van Der Laak, B. Van Ginneken, C.I. Sánchez, A survey on deep learning in medical image analysis, *Med. Image Anal.* 42 (2017) 60–88.
- [4] D. Shen, G. Wu, H.I. Suk, Deep learning in medical image analysis, *Annu. Rev. Biomed. Eng.* 19 (2017) 221–248.
- [5] V. Kajla, A. Gupta, A. Khatak, Analysis of x-ray images with image processing techniques: a review, in: 2018 4th International Conference on Computing Communication and Automation (ICCCA), IEEE, 2018, December, pp. 1–4.
- [6] J. Hsieh, B. Nett, Z. Yu, K. Sauer, J.B. Thibault, C.A. Bouman, Recent advances in CT image reconstruction, *Current Radiology Reports* 1 (2013) 39–51.
- [7] L.E. Crooks, An introduction to magnetic resonance imaging, *IEEE Eng. Med. Biol. Mag.* 4 (3) (1985) 8–15.
- [8] H. Ben Yedder, B. Cardoen, G. Hamarneh, Deep learning for biomedical image reconstruction: a survey, *Artif. Intell. Rev.* 54 (2021) 215–251.
- [9] S.H.S. Chou, G.A. Kicska, S.N. Pipavath, G.P. Reddy, Digital tomosynthesis of the chest: current and emerging applications, *Radiographics* 34 (2) (2014) 359–372.
- [10] I. Goodfellow, J. Pouget-Abadie, M. Mirza, B. Xu, D. Warde-Farley, S. Ozair, A. Courville, Y. Bengio, Generative adversarial nets, *Adv. Neural Inf. Process. Syst.* 27 (2014).
- [11] Khosro Bahrami, Feng Shi, Islem Rekik, Dinggang Shen, Convolutional neural network for reconstruction of 7T-like images from 3T MRI using appearance and anatomical features, in: Deep Learning and Data Labeling for Medical Applications: First International Workshop, LABELS 2016, and Second International Workshop, DLMIA 2016, Held in Conjunction with MICCAI 2016, Athens, Greece, October 21, 2016, Proceedings 1, Springer International Publishing, 2016, pp. 39–47.
- [12] D. Joo, D. Kim, J. Kim, Generating a fusion image: one's identity and another's shape, in: Proceedings of the IEEE Conference on Computer Vision and Pattern Recognition, 2018, pp. 1635–1643.
- [13] A. Gilbert, M. Marciniak, C. Rodero, P. Lamata, E. Samset, K. Mcleod, Generating synthetic labeled data from existing anatomical models: an example with echocardiography segmentation, *IEEE Trans. Med. Imag.* 40 (10) (2021) 2783–2794.
- [14] C. Li, M. Wand, Precomputed real-time texture synthesis with markovian generative adversarial networks, in: Computer Vision-ECCV 2016: 14th European Conference, Amsterdam, The Netherlands, October 11–14, 2016, Proceedings, Part III 14 (Pp. 702–716), Springer International Publishing, 2016.
- [15] X. Zhang, X. Zhu, N. Zhang, P. Li, L. Wang, Seggan: semantic segmentation with generative adversarial network, in: 2018 IEEE Fourth International Conference on Multimedia Big Data (BigMM), IEEE, 2018, September, pp. 1–5.
- [16] V. Thambawita, P. Salehi, S.A. Sheshkal, S.A. Hicks, H.L. Hammer, S. Parasra, T. D. Lange, P. Halvorsen, M.A. Riegler, SinGAN-Seg: synthetic training data generation for medical image segmentation, *PLoS One* 17 (5) (2022) e0267976.
- [17] A. Shokr, L.G. Pacheco, P. Thirumalaraju, M.K. Kanakasabapathy, J. Gandhi, D. Kartik, F.S. Silva, E. Erdogmus, H. Kundala, S. Luo, X.G. Yu, Mobile health (mHealth) viral diagnostics enabled with adaptive adversarial learning, *ACS Nano* 15 (1) (2020) 665–673.
- [18] O. Ergün, Y. Sahillioglu, 3D point cloud classification with ACGAN-3D and VACWGAN-GP, *Turk. J. Electr. Eng. Comput. Sci.* 31 (2) (2023) 381–395.
- [19] H. Zhang, T. Xu, H. Li, S. Zhang, X. Wang, X. Huang, D.N. Metaxas, Stackgan: text to photo-realistic image synthesis with stacked generative adversarial networks, in: Proceedings of the IEEE International Conference on Computer Vision, 2017, pp. 5907–5915.
- [20] X. Ying, H. Guo, K. Ma, J. Wu, Z. Weng, Y. Zheng, X2CT-GAN: reconstructing CT from biplanar X-rays with generative adversarial networks, in: Proceedings of the IEEE/CVF Conference on Computer Vision and Pattern Recognition, 2019, pp. 10619–10628.
- [21] Z. Wang, L. Wang, S. Duan, Y. Li, An image denoising method based on deep residual GAN, *J. Phys. Conf.* 1550 (3) (2020, May) 032127. IOP Publishing.
- [22] L. Galteri, L. Seidenari, M. Bertini, A. Del Bimbo, Deep generative adversarial compression artifact removal, in: Proceedings of the IEEE International Conference on Computer Vision, 2017, pp. 4826–4835.
- [23] E. Tzeng, J. Hoffman, K. Saenko, T. Darrell, Adversarial discriminative domain adaptation, in: Proceedings of the IEEE Conference on Computer Vision and Pattern Recognition, 2017, pp. 7167–7176.
- [24] X. Yi, E. Walia, P. Babyn, Generative adversarial network in medical imaging: a review, *Med. Image Anal.* 58 (2019) 101552.
- [25] J.J. Jeong, A. Tariq, T. Adejumo, H. Trivedi, J.W. Gichoya, I. Banerjee, Systematic review of generative adversarial networks (gans) for medical image classification and segmentation, *J. Digit. Imag.* 35 (2) (2022) 137–152.
- [26] A. Iqbal, M. Sharif, M. Yasmin, M. Raza, S. Aftab, Generative adversarial networks and its applications in the biomedical image segmentation: a comprehensive survey, *International Journal of Multimedia Information Retrieval* 11 (3) (2022) 333–368.
- [27] S. Xun, D. Li, H. Zhu, M. Chen, J. Wang, J. Li, M. Chen, B. Wu, H. Zhang, X. Chai, Z. Jiang, Generative adversarial networks in medical image segmentation: a review, *Comput. Biol. Med.* 140 (2022) 105063.
- [28] Y. Chen, X.H. Yang, Z. Wei, A.A. Heidari, N. Zheng, Z. Li, H. Chen, H. Hu, Q. Zhou, Q. Guan, Generative adversarial networks in medical image augmentation: a review, *Comput. Biol. Med.* 144 (2022) 105382.
- [29] E. Ferrante, N. Paragios, Slice-to-volume medical image registration: a survey, *Med. Image Anal.* 39 (2017) 101–123.
- [30] K. Wang, C. Gou, Y. Duan, Y. Lin, X. Zheng, F.Y. Wang, Generative adversarial networks: introduction and outlook, *IEEE/CAA Journal of Automatica Sinica* 4 (4) (2017) 588–598.
- [31] S. Cahyawijaya, Biomedical image reconstruction: a survey, *arXiv preprint arXiv:2301.11813* (2023).
- [32] R.J. Jaszczak, R.E. Coleman, C.B. Lim, SPECT: single photon emission computed tomography, *IEEE Trans. Nucl. Sci.* 27 (3) (1980) 1137–1153.
- [33] A.K. Shukla, U. Kumar, Positron emission tomography: an overview, *Journal of medical physics/Association of Medical Physicists of India* 31 (1) (2006) 13.
- [34] F.A.M. Cappabianco, C.S. Shida, J.S. Ide, Introduction to research in magnetic resonance imaging, in: 2016 29th SIBGRAPI Conference on Graphics, Patterns and Images Tutorials (SIBGRAPI-T), IEEE, 2016, October, p. 114.
- [35] A. Kanitsar, D. Fleischmann, R. Wegenkittl, D. Sandner, P. Felkel, E. Groller, Computed tomography angiography: a case study of peripheral vessel investigation, in: *Proceedings Visualization, 2001. VIS'01*, IEEE, 2001, October, pp. 477–493.
- [36] Z. Wang, Z. Cui, Y. Zhu, Multi-modal medical image fusion by Laplacian pyramid and adaptive sparse representation, *Comput. Biol. Med.* 123 (2020) 103823.
- [37] C.L. Chowdhary, D.P. Acharjya, Segmentation and feature extraction in medical imaging: a systematic review, *Procedia Comput. Sci.* 167 (2020) 26–36.
- [38] D. Huang, E.A. Swanson, C.P. Lin, J.S. Schuman, W.G. Stinson, W. Chang, M. R. Hee, T. Flotte, K. Gregory, C.A. Puliafito, J.G. Fujimoto, Optical coherence tomography, *Science* 254 (5035) (1991) 1178–1181.
- [39] X. Zhang, Y. Sugano, M. Fritz, A. Bulling, Appearance-based gaze estimation in the wild, in: *Proceedings of the IEEE Conference on Computer Vision and Pattern Recognition*, 2015, pp. 4511–4520.
- [40] E. Wood, T. Baltrusaitis, L.P. Morency, P. Robinson, A. Bulling, Learning an appearance-based gaze estimator from one million synthesised images, in: *Proceedings of the Ninth Biennial ACM Symposium on Eye Tracking Research & Applications*, 2016, March, pp. 131–138.
- [41] P. Isola, J.Y. Zhu, T. Zhou, A.A. Efros, Image-to-image translation with conditional adversarial networks, in: *Proceedings of the IEEE Conference on Computer Vision and Pattern Recognition*, 2017, pp. 1125–1134.
- [42] H. Zhang, T. Xu, H. Li, S. Zhang, X. Wang, X. Huang, D.N. Metaxas, Stackgan: text to photo-realistic image synthesis with stacked generative adversarial networks, in: *Proceedings of the IEEE International Conference on Computer Vision*, 2017, pp. 5907–5915.
- [43] J.Y. Zhu, T. Park, P. Isola, A.A. Efros, Unpaired image-to-image translation using cycle-consistent adversarial networks, in: *Proceedings of the IEEE International Conference on Computer Vision*, 2017, pp. 2223–2232.
- [44] C. Ledig, L. Theis, F. Huszár, J. Caballero, A. Cunningham, A. Acosta, A. Aitken, A. Tejani, J. Totz, Z. Wang, W. Shi, Photo-realistic single image super-resolution using a generative adversarial network, in: *Proceedings of the IEEE Conference on Computer Vision and Pattern Recognition*, 2017, pp. 4681–4690.
- [45] G. Perarnau, J. Van De Weijer, B. Raducanu, J.M. Alvarez, Invertible conditional gans for image editing, *arXiv preprint arXiv:1611.06355* (2016).
- [46] B. Zhao, B. Chang, Z. Jie, L. Sigal, Modular generative adversarial networks, in: *Proceedings of the European Conference on Computer Vision, ECCV*, 2018, pp. 150–165.
- [47] T. Karras, S. Laine, T. Aila, A style-based generator architecture for generative adversarial networks, in: *Proceedings of the IEEE/CVF Conference on Computer Vision and Pattern Recognition*, 2019, pp. 4401–4410.
- [48] S. Motamed, P. Rogalla, F. Khalvati, RANDGAN: randomized generative adversarial network for detection of COVID-19 in chest X-ray, *Sci. Rep.* 11 (1) (2021) 8602.
- [49] W. Li, P. Zhang, L. Zhang, Q. Huang, X. He, S. Lyu, J. Gao, Object-driven text-to-image synthesis via adversarial training, in: *Proceedings of the IEEE/CVF Conference on Computer Vision and Pattern Recognition*, 2019, pp. 12174–12182.
- [50] M. Wiatrak, S.V. Albrecht, A. Nystrom, Stabilizing generative adversarial networks: a survey, *arXiv preprint arXiv:1910.00927* (2019).
- [51] N.T. Tran, T.A. Bui, N.M. Cheung, Dist-gan: an improved gan using distance constraints, in: *Proceedings of the European Conference on Computer Vision, ECCV*, 2018, pp. 370–385.
- [52] N. Kodali, J. Abernethy, J. Hays, Z. Kira, On convergence and stability of gans, *arXiv preprint arXiv:1705.07215* (2017).
- [53] Z. Lin, A. Khetan, G. Fanti, S. Oh, Pacgan: the power of two samples in generative adversarial networks, *Adv. Neural Inf. Process. Syst.* 31 (2018).
- [54] G. Klambauer, T. Unterthiner, A. Mayr, S. Hochreiter, Self-normalizing neural networks, *Adv. Neural Inf. Process. Syst.* 30 (2017).
- [55] T. Miyato, T. Kataoka, M. Koyama, Y. Yoshida, Spectral normalization for generative adversarial networks, *arXiv preprint arXiv:1802.05957* (2018).
- [56] L. Metz, B. Poole, D. Pfau, J. Sohl-Dickstein, Unrolled generative adversarial networks, *arXiv preprint arXiv:1611.02163* (2016).
- [57] T. Motwani, M. Parmar, A Novel Framework for Selection of GANs for an Application, 2020 *arXiv preprint arXiv:2002.08641*.

- [58] J. Sohl-Dickstein, E. Weiss, N. Maheswaranathan, S. Ganguli, Deep unsupervised learning using nonequilibrium thermodynamics, in: International Conference on Machine Learning, PMLR, 2015, June, pp. 2256–2265.
- [59] J. Ho, A. Jain, P. Abbeel, Denoising diffusion probabilistic models, *Adv. Neural Inf. Process. Syst.* 33 (2020) 6840–6851.
- [60] A. Güngör, S.U. Dar, Ş. Öztürk, Y. Korkmaz, H.A. Bedel, G. Elmas, T. Çukur, Adaptive diffusion priors for accelerated MRI reconstruction, *Med. Image Anal.* 88 (2023) 102872.
- [61] M. Özbeý, O. Dalmaz, S.U. Dar, H.A. Bedel, Ş. Öztürk, A. Güngör, T. Çukur, Unsupervised medical image translation with adversarial diffusion models, *IEEE Trans. Med. Imaging* 42 (12) (2023) 3524–3539.
- [62] W. Wu, J. Pan, Y. Wang, S. Wang, J. Zhang, Multi-channel optimization generative model for stable ultra-sparse-view CT reconstruction, *IEEE Trans. Med. Imaging* 43 (10) (2024) 3461–3475.
- [63] J. Zhang, H. Mao, X. Wang, Y. Guo, W. Wu, Wavelet-inspired multi-channel score-based model for limited-angle CT reconstruction, *IEEE Trans. Med. Imaging* 43 (10) (2024) 3436–3448.
- [64] Briony J. Oates, Researching Informationsystems and Computing, vol. 1, SAGE Publications, 2006, pp. 93–107. Ltd1 Oliver's Yard55 City RoadLondon EC1Y 1SP, ISSN: 1-4129-0223-1, 1-4129-0224-X (pbk).
- [65] N.R. Haddaway, M.J. Page, C.C. Pritchard, L.A. McGuinness, PRISMA2020: an R package and Shiny app for producing PRISMA 2020-compliant flow diagrams, with interactivity for optimised digital transparency and Open Synthesis, *Campbell systematic reviews* 18 (2) (2022) e1230.
- [66] J. Zhang, X. He, L. Qing, F. Gao, B. Wang, BPGAN: brain PET synthesis from MRI using generative adversarial network for multi-modal Alzheimer's disease diagnosis, *Comput. Methods Progr. Biomed.* 217 (2022) 106676.
- [67] X. Wang, M. Zheng, COVID-19 image segmentation algorithms based on conditional generative adversarial network, in: Proceedings of the 2022 5th International Conference on Artificial Intelligence and Pattern Recognition, 2022, September, pp. 419–426.
- [68] D. Qiu, Y. Cheng, X. Wang, Improved generative adversarial network for retinal image super-resolution, *Comput. Methods Progr. Biomed.* 225 (2022) 106995.
- [69] M. Molahasani Majdabadi, Y. Choi, S. Deivalakshmi, S. Ko, Capsule GAN for prostate MRI super-resolution, *Multimed. Tool. Appl.* 81 (3) (2022) 4119–4141.
- [70] X. Wu, L. Bi, M. Fulham, D.D. Feng, L. Zhou, J. Kim, Unsupervised brain tumor segmentation using a symmetric-driven adversarial network, *Neurocomputing* 455 (2021) 242–254.
- [71] Z. Wang, A.C. Bovik, H.R. Sheikh, E.P. Simoncelli, Image quality assessment: from error visibility to structural similarity, *IEEE Trans. Image Process.* 13 (4) (2004) 600–612.
- [72] J. Zhang, X. He, L. Qing, F. Gao, B. Wang, BPGAN: brain PET synthesis from MRI using generative adversarial network for multi-modal Alzheimer's disease diagnosis, *Comput. Methods Progr. Biomed.* 217 (2022) 106676.
- [73] U. Sarra, Comparative study of different quality assessment techniques on color images, *Iconic Res. Eng* 2 (2019) 127–133.
- [74] D.J. Hemanth, D. Gupta, V.E. Balas (Eds.), *Intelligent Data Analysis for Biomedical Applications: Challenges and Solutions*, Academic Press, 2019.
- [75] S.A. Hicks, I. Strümke, V. Thambawita, M. Hammou, M.A. Riegler, P. Halvorsen, S. Parasuraman, On evaluation metrics for medical applications of artificial intelligence, *Sci. Rep.* 12 (1) (2022) 5979.
- [76] E. Ahishakiye, M. Bastiaan Van Gijzen, J. Tumwiine, R. Wario, J. Obungoloch, A survey on deep learning in medical image reconstruction, *Intelligent Medicine* 1 (3) (2021) 118–127.
- [77] G. Yang, S. Yu, H. Dong, G. Slabaugh, P.L. Dragotti, X. Ye, D. Firmin, DAGAN: deep de-aliasing generative adversarial networks for fast compressed sensing MRI reconstruction, *IEEE Trans. Med. Imag.* 37 (6) (2017) 1310–1321.
- [78] T. Zhou, Q. Li, H. Lu, Q. Cheng, X. Zhang, GAN review: models and medical image fusion applications, *Inf. Fusion* 91 (2023) 134–148.
- [79] K. Suganthi, Review of medical image synthesis using GAN techniques, in: *ITM Web of Conferences*, vol. 37, EDP Sciences, 2021 01005.
- [80] D. Avola, L. Cinque, A. Fagioli, G. Foresti, A. Mecca, Ultrasound medical imaging techniques: a survey, *ACM Comput. Surv.* 54 (3) (2021) 1–38.
- [81] Y. Fu, Y. Lei, T. Wang, W.J. Curran, T. Liu, X. Yang, Deep learning in medical image registration: a review, *Phys. Med. Biol.* 65 (20) (2020) 20TR01.
- [82] C. Tanner, F. Ozdemir, R. Profanter, V. Vishnevsky, E. Konukoglu, O. Goksel, Generative adversarial networks for MR-CT deformable image registration, *arXiv preprint arXiv:1807.07349* (2018).
- [83] C. Shorten, T.M. Khoshgoftaar, A survey on image data augmentation for deep learning, *Journal of big data* 6 (1) (2019) 1–48.
- [84] Y. Chen, X.H. Yang, Z. Wei, A.A. Heidar, N. Zheng, Z. Li, Q. Guan, Generative adversarial networks in medical image augmentation: a review, *Comput. Biol. Med.* 144 (2022) 105382.
- [85] J. Ouyang, G. Wang, E. Gong, K. Chen, J. Pauly, G. Zaharchuk, Task-GAN: improving generative adversarial network for image reconstruction, in: *Machine Learning for Medical Image Reconstruction: Second International Workshop, MLMIR 2019, Held in Conjunction with MICCAI 2019, Shenzhen, China, October 17, 2019, Proceedings 2* (Pp. 193–204), Springer International Publishing, 2019.
- [86] X. Jiang, M. Liu, F. Zhao, X. Liu, H. Zhou, A novel super-resolution CT image reconstruction via semi-supervised generative adversarial network, *Neural Comput. Appl.* 32 (2020) 14563–14578.
- [87] H. Lan, K. Zhou, C. Yang, J. Cheng, J. Liu, S. Gao, F. Gao, Ki-GAN: knowledge infusion generative adversarial network for photoacoustic image reconstruction *in vivo*, in: *Medical Image Computing and Computer Assisted Intervention—MICCAI 2019: 22nd International Conference, Shenzhen, China, October 13–17, 2019, Proceedings, Part I* 22 (Pp. 273–281), Springer International Publishing, 2019.
- [88] K. Guo, X. Hu, X. Li, MMFGAN: a novel multimodal brain medical image fusion based on the improvement of generative adversarial network, *Multimed. Tool. Appl.* 81 (4) (2022) 5889–5927.
- [89] Y. Gu, Z. Zeng, H. Chen, J. Wei, Y. Zhang, B. Chen, Y. Lu, MedSRGAN: medical images super-resolution using generative adversarial networks, *Multimed. Tool. Appl.* 79 (2020) 21815–21840.
- [90] D. Qiu, Y. Cheng, X. Wang, Improved generative adversarial network for retinal image super-resolution, *Comput. Methods Progr. Biomed.* 225 (2022) 106995.
- [91] G. Wang, X. Hu, Low-dose CT denoising using a progressive wasserstein generative adversarial network, *Comput. Biol. Med.* 135 (2021) 104625.
- [92] G. Wang, E. Gong, S. Banerjee, J. Pauly, G. Zaharchuk, Accelerated MRI reconstruction with dual-domain generative adversarial network, in: *Machine Learning for Medical Image Reconstruction: Second International Workshop, MLMIR 2019, Held in Conjunction with MICCAI 2019, Shenzhen, China, October 17, 2019, Proceedings 2* (Pp. 47–57), Springer International Publishing, 2019.
- [93] B. Murugesan, S. Vijaya Raghavan, K. Sarveswaran, K. Ram, M. Sivaprasakam, Recon-GLGAN: a global-local context based generative adversarial network for MRI reconstruction, in: *Machine Learning for Medical Image Reconstruction: Second International Workshop, MLMIR 2019, Held in Conjunction with MICCAI 2019, Shenzhen, China, October 17, 2019, Proceedings 2* (Pp. 3–15), Springer International Publishing, 2019.
- [94] Jiahao Huang, Weiping Ding, Jun Lv, Jingwen Yang, Hao Dong, Javier Del Ser, Jun Xia, Tiaojuan Ren, Stephen T. Wong, Guang Yang, Edge-enhanced dual discriminator generative adversarial network for fast MRI with parallel imaging using multi-view information, *Appl. Intell.* 52 (13) (2022) 14693–14710.
- [95] H. Li, Z. Xuan, J. Zhou, X. Hu, B. Yang, Fast and accurate super-resolution of MR images based on lightweight generative adversarial network, *Multimed. Tool. Appl.* 82 (2) (2023) 2465–2487.
- [96] S. Kyung, J. Won, S. Pak, G.S. Hong, N. Kim, MTD-GAN: multi-task discriminator based generative adversarial networks for low-dose CT denoising, in: *International Workshop on Machine Learning for Medical Image Reconstruction*, Springer International Publishing, Cham, 2022, September, pp. 133–144.
- [97] X. Zhao, T. Yang, B. Li, X. Zhang, SwinGAN: a dual-domain Swin Transformer-based generative adversarial network for MRI reconstruction, *Comput. Biol. Med.* 153 (2023) 106513.
- [98] S. Poonkodi, M. Kanchana, 3D-MedTranCSGAN: 3D medical image transformation using CSGAN, *Comput. Biol. Med.* 153 (2023) 106541.
- [99] N. Pradhan, V.S. Dhaka, G. Rani, H. Chaudhary, Transforming view of medical images using deep learning, *Neural Comput. Appl.* 32 (18) (2020) 15043–15054.
- [100] Y. Luo, Y. Wang, C. Zu, B. Zhan, X. Wu, J. Zhou, L. Zhou, 3D transformer-GAN for high-quality PET reconstruction, in: *Medical Image Computing and Computer Assisted Intervention—MICCAI 2021: 24th International Conference, Strasbourg, France, September 27–October 1, 2021, Proceedings, Part VI* 24, Springer International Publishing, 2021, pp. 276–285.
- [101] X. Wu, L. Bi, M. Fulham, D.D. Feng, L. Zhou, J. Kim, Unsupervised brain tumor segmentation using a symmetric-driven adversarial network, *Neurocomputing* 455 (2021) 242–254.
- [102] S. Chen, S. Sun, X. Huang, D. Shen, Q. Wang, S. Liao, Data-consistency in latent space and online update strategy to guide GAN for fast MRI reconstruction, in: *Machine Learning for Medical Image Reconstruction: Third International Workshop, MLMIR 2020, Held in Conjunction with MICCAI 2020, Lima, Peru, October 8, 2020, Proceedings 3*, Springer International Publishing, 2020, pp. 82–90.
- [103] A. Khan, W. Jin, R.A. Naqvi, Perceptual adversarial non-residual learning for blind image denoising, *Soft Comput.* 26 (16) (2022) 7933–7957.
- [104] H. Xie, T. Zhang, W. Song, S. Wang, H. Zhu, R. Zhang, Y. Zhao, Super-resolution of *Pneumocystis carinii* pneumonia CT via self-attention GAN, *Comput. Methods Progr. Biomed.* 212 (2021) 106467.
- [105] S. Shivatekar, J. Mangalagiri, P. Nguyen, D. Chapman, M. Haleem, R. Gite, An intelligent parallel distributed streaming framework for near real-time science sensors and high-resolution medical images, in: *50th International Conference on Parallel Processing Workshop*, 2021, August, pp. 1–9.
- [106] Y. Huang, Q. Wang, S. Omachi, Rethinking degradation: radiograph super-resolution via aid-gan, in: *International Workshop on Machine Learning in Medical Imaging*, Springer Nature Switzerland, Cham, 2022, September, pp. 43–52.
- [107] K. Zhou, Y. Xiao, J. Yang, J. Cheng, W. Liu, W. Luo, S. Gao, Encoding structure-texture relation with p-net for anomaly detection in retinal images, in: *Computer Vision—ECCV 2020: 16th European Conference, Glasgow, UK, August 23–28, 2020, Proceedings, Part XX* 16, Springer International Publishing, 2020, pp. 360–377.
- [108] X. Gu, Y. Zhang, W. Zeng, S. Zhong, H. Wang, D. Liang, Z. Hu, Cross-modality image translation: CT image synthesis of MR brain images using multi generative network with perceptual supervision, *Comput. Methods Progr. Biomed.* 237 (2023) 107571.
- [109] R. Fang, R. Guo, M. Zhao, M. Yao, Low-count PET image reconstruction algorithm based on WGAN-GP, in: *Proceedings of the 2023 3rd International Conference on Bioinformatics and Intelligent Computing*, 2023, February, pp. 60–64.